SARS-CoV-2 transmission across age groups in France and implications for control

Cécile Tran Kiem, Paolo Bosetti, Juliette Paireau, Pascal Crepey, Henrik Salje, Noémie Lefrancq, Arnaud Fontanet, Daniel Benamouzig, Pierre-Yves Boëlle, Jean-Claude Desenclos, et al.

SARS-CoV-2 transmission across age groups in France and implications for control

Cécile Tran Kiem[1,2], Paolo Bosetti[1], Juliette Paireau[1,3], Pascal Crépey[4], Henrik Salje[1,5], Noémie Lefrancq[1,5], Arnaud Fontanet[6,7], Daniel Benamouzig[8], Pierre-Yves Boëlle[9], Jean-Claude Desenclos[3], Lulla Opatowski[10,11], Simon Cauchemez[1]

Affiliations:

1. Mathematical Modelling of Infectious Diseases Unit, Institut Pasteur, UMR2000, CNRS, Paris, France
2. Collège Doctoral, Sorbonne Université, Paris, France
3. Santé publique France, French National Public Health Agency, Saint-Maurice, France
4. Univ Rennes, EHESP, REPERES « Recherche en Pharmaco-Epidémiologie et Recours aux Soins » – EA 7449, Rennes, France
5. Department of Genetics, University of Cambridge, Cambridge, UK
6. Emerging Diseases Epidemiology Unit, Institut Pasteur, Paris, France
7. PACRI Unit, Conservatoire National des Arts et Métiers, Paris, France
8. Sciences Po - Centre de sociologie des organisations and Chaire santé - CNRS, Paris, France
9. Sorbonne Université, INSERM, Institut Pierre Louis d'Epidémiologie et de Santé Publique, Paris, France
10. Institut Pasteur, Epidemiology and Modelling of Antibiotic Evasion (EMAE), Paris, France
11. Université Paris-Saclay, UVSQ, Inserm, CESP, Anti-infective evasion and pharmacoepidemiology team, Montigny-Le-Bretonneux, France

Short titles: Transmission of SARS-CoV-2 across ages

One-sentence summary: The porosity of SARS-CoV-2 transmission across ages reveals the impracticability of strategies shielding at-risk individuals.

Corresponding author: Simon Cauchemez, Mathematical Modelling of Infectious Diseases Unit, Institut Pasteur, 28 rue du Dr Roux, 75015, Paris, France, simon.cauchemez@pasteur.fr

Abstract

The shielding of older individuals has been proposed to limit COVID-19 hospitalizations while relaxing general social distancing. Evaluating such approaches requires a deep understanding of transmission dynamics across ages. Here, we use detailed age-specific case and hospitalization data to model the rebound in the French epidemic in summer 2020, characterize age-specific transmission dynamics and critically evaluate different age-targeted intervention measures. We find that while the rebound started in young adults, it reached individuals aged >80 y.o. after 4 weeks, indicating substantial porosity across ages. We derive from these patterns the contribution of each age group to transmission. While shielding older individuals reduces morbi-mortality, it is insufficient to allow major relaxations of social distancing. When the epidemic remains manageable (R close to 1), targeting those that contribute more to transmission is better than shielding at-risk individuals. Pandemic control requires an effort from all age groups.

Main

To mitigate the impact of the SARS-CoV-2 pandemic, many countries implemented drastic social distancing measures that proved effective at reducing the stress on the healthcare system (*1*, *2*) but have been associated with major social and economic costs because they require an effort from all. Since infections leading to hospitalization and death are concentrated in elderly people and people with comorbidities, some have argued that strategies that shield at-risk individuals from infection (for example by isolating them) could be used to maintain hospitalizations at low levels while relaxing costly social distancing measures that affect the rest of society (*3*). These arguments resonate with decades-old debates on the relative contribution to disease control of strategies that target at-risk individuals versus disease transmitters (*4*–*9*).

To determine whether such strategies may allow the relaxation of social distancing measures, it is essential to robustly evaluate the dynamics of transmission of SARS-CoV-2 across age groups. The epidemic rebound that occurred in France in the summer-autumn of 2020 offers the perfect opportunity to do this. The nationwide lockdown implemented in spring 2020 (*1*) was followed by the progressive relaxation of social distancing measures, the scaling up of a strategy based on testing, contact tracing and case isolation and the general use of face masks. However, this did not impede a large second wave in the autumn and a new lockdown in November 2020.

Here, we build a modeling framework to reconstruct the complex patterns of spread of SARS-CoV-2 across age groups along with the dynamics of infections and hospitalizations, from the detailed analysis of age-stratified case (N=368,906) and hospitalization (N=16,548) data from all 13 regions of Metropolitan France, between 15 June and 28 September 2020. We fit our model to age-stratified hospital admissions and the incidence of infection among symptomatic individuals that received a RT-PCR test result (labelled symptomatic individuals in the rest of the text). Based on these dynamics, it is possible to quantify the relative contribution of each age group to transmission by estimating the ratio of the average number of daily contacts that are effective for transmission in each age group, relative to those aged 20-29 years-old (y.o.) (reference group). This characterization can then be used to critically evaluate different age-targeted intervention measures. We first detail the results for Auvergne-Rhône-Alpes (8 million inhabitants), which was one of the first regions to experience an epidemic rebound (Figure S1); and then present results for all 13 regions in metropolitan France.

In the Auvergne-Rhône-Alpes region, the proportion of positive tests among symptomatic individuals aged 20-29 y.o. increased from 3.4% to 13.8% between 27 July 2020 and 17 August 2020 (Figure 1A). This increase was quickly followed by a rise in incidence (Figure 1A, 1B) and hospital admissions in other age groups (Figure 1C, 1D). For example, in the week of 14 September 2020, 14.6% of symptomatic individuals aged >80 y.o. were

positive (compared to 1.1% on the week of 17 August 2020) and there were 169 hospital admissions of patients in that age group (compared to 23 on the week of 17 August 2020). These trends were observed across all metropolitan French regions, with a mean lag of 4 weeks between the increase in the proportion of positive tests among symptomatic individuals aged 20-29 y.o. and those older than 80 y.o. (Figure 1E). This indicates substantial porosity of transmission between age groups.

Fitting our model to these data, we estimate that, in Auvergne-Rhône-Alpes, the basic reproduction number R_0 increased from 0.68 during the lockdown to 0.87 [0.86 - 0.88] between 11 May and 8 July and to 1.37 [1.36 - 1.37] from 9 July to 28 September 2020 (Figure 2A, Table S1). We estimate that the number of effective contacts in the rebound period starting on 9 July was the highest in individuals aged 20-29 y.o (Figure 2B). As a comparison, the number of effective contacts in those aged 50-59 y.o. and >80 y.o. was respectively 0.87 [0.85 - 0.90] and 0.54 [0.51 - 0.57] times the effective contacts in individuals aged 20-29 y.o. These estimates are largely consistent with the number of daily contacts measured in different age groups by the online survey SocialCov (30 July-27 September 2020) (see Supplementary Information) (*10*), but for two key differences (Figure 2B). First, we estimated that the number of effective contacts for transmission in children was substantially lower than the reported number of contacts in the survey. This reflects the limited contribution of children to SARS-CoV-2 transmission, especially the youngest ones, during this time period and is consistent with either a lower susceptibility to SARS-CoV-2 infection or a reduced infectivity compared to older individuals (*11*, *12*). Second, the contribution to transmission of those aged 30-49 y.o. relative to those aged 20-29 y.o. is about 25% lower than what might be expected from the contact survey. Again, this might be explained by reduced risks of transmission given contact, for example thanks to better compliance with the use of masks or physical distancing. These differences highlight the distinction between raw contacts measured from contact surveys and effective contacts that we estimate and that also capture different risks of transmission given contact. Our estimated mixing patterns can reproduce the observed rises in incidence (Figure 2C-E, Figure S2, Figure S3) and hospital admissions by age group (Figure 2F-H, Figure S2, Figure S4).

We use our model to assess the potential impact of social distancing measures targeting different age groups. To simplify presentation, we derive the average number of effective contacts for each age group from our age-specific estimates of the relative contribution to transmission (Figure 2B), under the assumption that the number of effective contacts for those aged 20-29 y.o. is equal to 7.7 contacts per day, as was measured in the SovialCov survey. We further assume that when individuals reduce their contacts, this affects all their contacts homogeneously.

In Auvergne-Rhône-Alpes, the effective reproduction number R_{eff} increased from 1.3 to 1.5 during the build up of the Autumn wave (*13*–*15*). Even though this corresponds to a

50% reduction in the transmission rate compared to a scenario with no control measures (*1*), this was insufficient to avoid a surge in hospitalizations and eventually the implementation of a national lockdown on 30 October 2020. We explore whether shielding individuals aged ≥70 y.o. could have been sufficient to maintain the epidemic at manageable levels for hospitalizations while relaxing control measures so that the effective reproduction ratio would be R_{eff}≥1.3-1.5. We deliberately consider an "extreme" scenario of shielding where the number of effective contacts of the target age group would be reduced by 50% to be similar to what was measured during the lockdown of March-May 2020 (*10*). Going further than this reduction seems difficult as this lockdown was already very strict. We find that in the range R_{eff} = 1.3-1.5, this would still result in 68-158 per million daily hospital admissions at the peak, above the national peak of March-April 2020 (56 per million) (Figure 3A) and 644-1028 deaths per million (Figure 3B). Further relaxing control measures up to R_{eff}=1.8 would increase the peak daily number of hospitalized patients to 320 per million and the overall number of deaths to 1516 per million.

This suggests that shielding at-risk individuals would not allow an important relaxation of social distancing measures as the reproduction number needs to be maintained close to 1 for the epidemic to remain manageable. This requires efforts from all age groups. In this latter context of a slowly growing epidemic characterized by R_{eff} close to 1, we investigate if it would be better from a public health perspective to reduce contacts of at-risk individuals rather than those of other age groups. We find that, for R_{eff} close to 1, targeting 20-29 y.o. individuals, i.e. the age-group with the largest number of effective contacts, results in the largest reduction in key epidemiological metrics. For example, considering the example of the region Auvergne-Rhône-Alpes, in a scenario where $R_{eff} = 1.1$, the peaks in new infections (Figure 4A), hospital admissions (Figure 4B) and ICU admissions (Figure 4C) and the number of deaths (Figure 4D) would drop by 44%, 43%,43% and 37%, respectively, if all individuals aged 20-29 y.o. reduced their average number of effective contacts by 1 (i.e. from 7.7 contacts per day to 6.7 on average), compared to 9%, 17%, 11% and 22%, respectively, if those aged >80 y.o. were targeted instead (from 4.2 to 3.2 contacts per day on average).

We found above that the healthcare system would be unable to cope with large values of the reproduction number even if at-risk individuals were shielded. We nevertheless explore such scenarios in case the cost of control measures was judged too elevated by decision makers. As the reproduction number increases, the same efforts in terms of reductions of contacts would lead to lower impact on key epidemiological metrics; and the ordering of strategies may change. Targeting >80 y.o. individuals becomes the best strategy to reduce deaths when R_{eff} is >1.21 (Figure 4D). For instance, if $R_{eff} = 1.6$, the number of deaths would drop by 15% if we removed 1 effective contact for those aged >80 y.o.; but by only 5% if we targeted those aged 20-29 y.o. We find a similar pattern if

the objective is to minimize the number of life-years lost and quality-adjusted life years (Figure S5). For large values of R_{eff}, we obtain relative similar reductions on peak hospital admissions irrespective of the target group among all age groups >20 y.o. To reduce peak ICU admission, it remains slightly less interesting to target those aged >80 y.o. since this population is less likely to be admitted in ICU. Targeting those that contribute most to transmission always provides the largest reduction in the peak number of infections irrespective of the value of R_{eff}. These conclusions remain unchanged when a larger number of effective contacts is being removed, although the impact on epidemiological metrics increases (Figure S6-S7).

As the number of effective contacts differs between age groups (Figure 2B), a reduction of 1 effective contact does not correspond to the same effort in the different age groups. For example, removing 1 effective contact per day corresponds to a 13% reduction of contacts in individuals aged 20-29 y.o., but a 24% reduction in those aged >80 y.o. Applying the same 20% reduction of effective contacts in all age groups, we find that the largest reduction in the peak of new infections, hospital admissions and ICU admissions is obtained when targeting the 20-29 y.o. regardless of the effective reproduction number value (Figure S8). The optimal strategy to minimize the number of deaths targets those aged >80 y.o. when $R_{eff} > 1.41$ (compared to >1.21 for an absolute reduction of 1 contact) (Figure S9).

Our model can reproduce the dynamics of test positivity in symptomatic individuals and hospitalizations across all the regions of metropolitan France (Figure S10-S21). We also find consistent patterns regarding the numbers of effective contacts by age group across regions (Figure S22), with the highest values observed in individuals aged 20-29 y.o. Considering data from other regions, we reach the same conclusion that in situations characterized by R_{eff} close to 1 where the epidemic may remain manageable, it is particularly beneficial to reduce effective contacts of those that contribute the most to transmission; while for larger values of R_{eff} that are likely to lead to a major crisis in hospitals, it is optimal to target those with the highest risk of severe outcome (Figure 4E-H, Figure S5).

At the start of the Autumn wave, we observed a very consistent epidemiological pattern across the 13 regions of metropolitan France. It started with an increase of infections among young adults, that was followed up by a rise in infections in other age groups and eventually in older individuals. Similar patterns have been observed in other locations (*16*). This indicates substantial porosity of transmission across age groups. We used our model to quantify this phenomenon and derive an evaluation of control strategies targeting different age groups. We found that even if we managed to reduce effective contacts of older individuals by 50%, this would not allow important relaxations of control measures. In practice, it is unclear whether it would be possible to achieve such

reductions for this age group since i) older individuals already behave very carefully with a number of effective contacts that is almost twice lower than that of those aged 20-29 y.o and ii) they are often dependent persons whose contacts are required for their basic daily activities. In all instances, our results indicate that to avoid a major crisis in hospitals, it is essential to maintain transmission rates at relatively low levels (with R_{eff} close to 1) which requires efforts from all. For this parameter regime where R_{eff} is close to 1, reducing contacts in younger age groups who contribute more to transmission would have a larger impact on key epidemiological indicators than targeting at-risk individuals.

Besides, strategies based on shielding a single part of the population, like the elderly, may raise serious ethical and social concerns. Such strategies can easily fuel societal controversies undermining social cohesion ("age-itation"), often viewed as a key asset in the management of the epidemic (*17*, *18*). Differentiated strategies might also modify the compliance of certain groups to other measures, which could reduce their impact. From a broader social perspective, the focus on the elderly would also represent a breach in values of solidarity between citizens and generations, which is considered as a cement of the welfare state in countries like France. The isolation of the elderly would erode social ties and weaken their situation, with strong concerns on ethical principles such as autonomy and benevolence (*19*). From a wider political perspective, such strategies would also represent a shift in the legitimacy of the State to intervene to control the epidemic: by promoting self-protection strategies rather than collective measures, governments will weaken their own capacity to intervene, leaving ground to more individualistic strategies.

While shielding older individuals can reduce COVID-19 mortality and morbidity, the intervention would not allow an important relaxation of control measures for other age groups due to the porosity of SARS-CoV-2 transmission across age groups. Pandemic control requires an effort from all age groups.

Figures

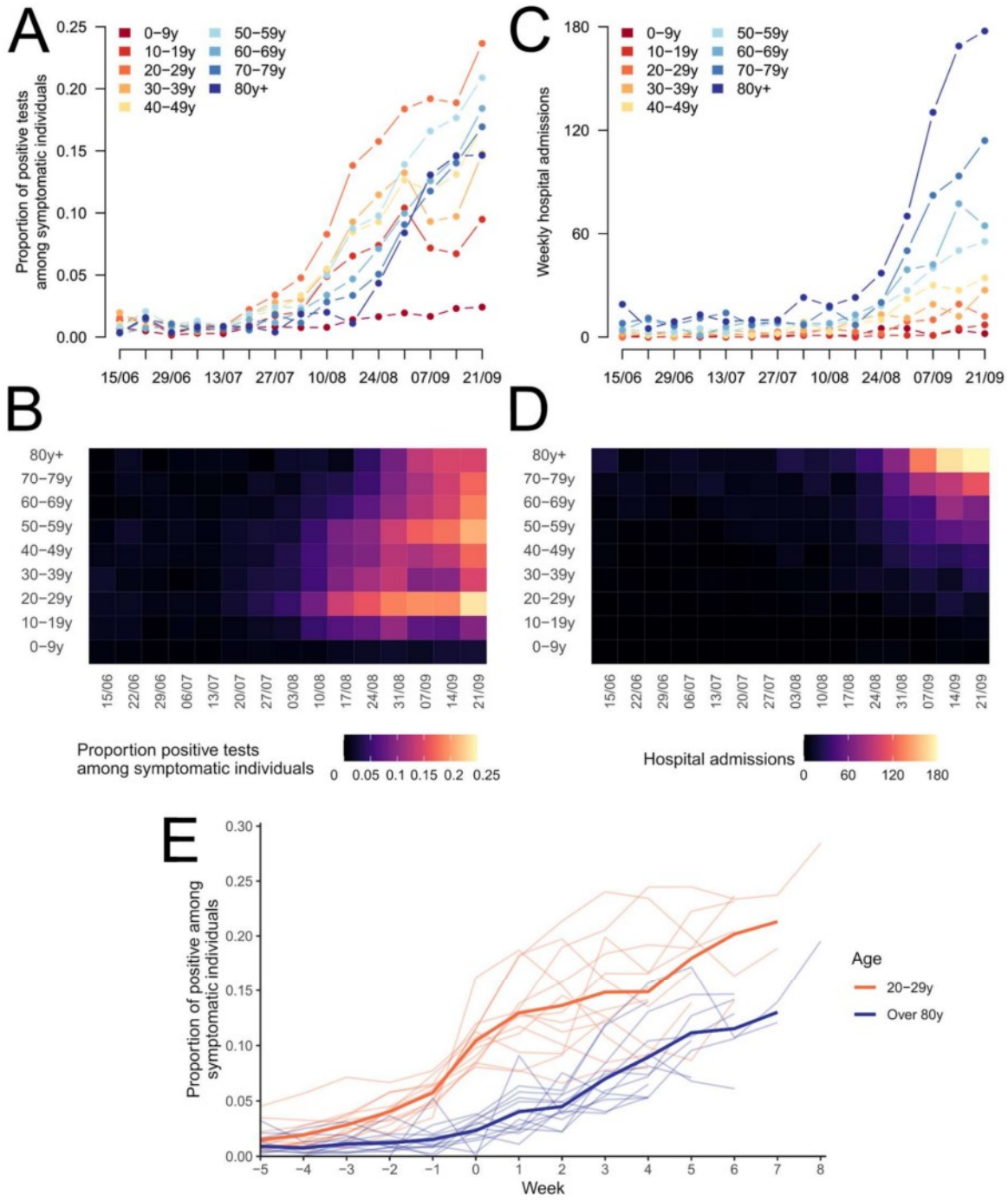

Figure 1: Dynamics of the epidemic rebound by age-group. **(A-B)** Weekly proportion of positive tests amongst symptomatic individuals being tested and **(C-D)** weekly number of hospital admissions, by age group in Auvergne-Rhône-Alpes region. **(E)** Proportion of

positive tests among symptomatic individuals in individuals aged 20-29 y.o. and older than 80 y.o. In (E), the light lines represent the trends in the 13 metropolitan French regions. The wider lines indicate the mean proportion of positive among symptomatic across regions. Week 0 corresponds to the first week when the proportion of positive tests among symptomatic individuals aged 20-29 y.o. reaches 8%.

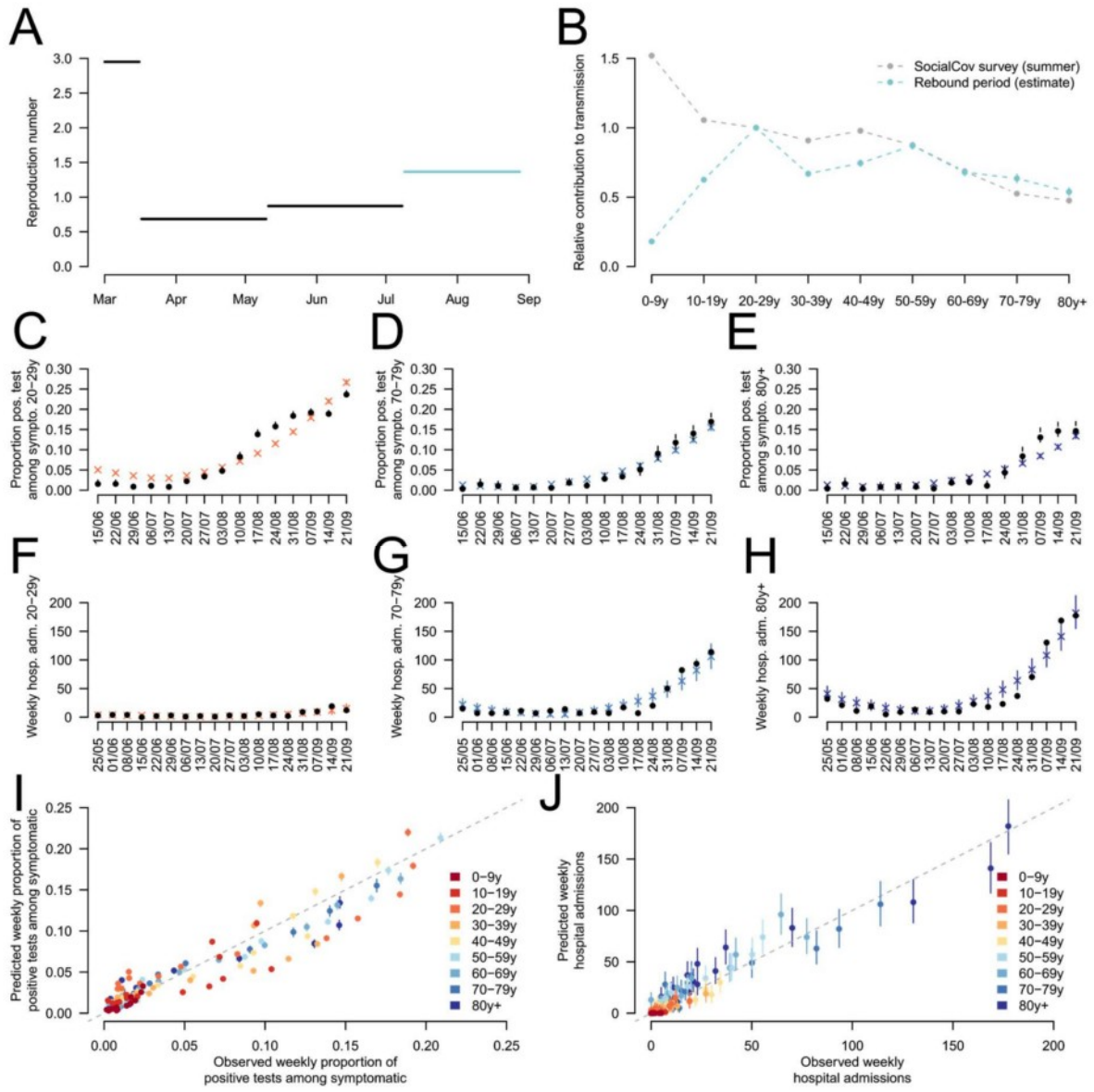

Figure 2: Model predictions for Auvergne-Rhône-Alpes region. (A) Basic reproduction number estimates during the epidemic. **(B)** Relative contribution of each age group to transmission during the rebound period (9 July - 27 September) compared to the reference group (20-29 y.o.). Predicted and observed weekly proportion of positive tests amongst symptomatic individuals being tested aged **(C)** 20-29y, **(D)** 70-79y and **(E)** 80y+. Predicted and observed weekly number of hospitalizations of individuals aged **(F)** 20-29y, **(G)** 70-79y and **(H)** 80y+. **(I)** Predicted and observed weekly proportion of positive tests among symptomatic individuals being tested. **(J)** Predicted and observed weekly hospital admissions. The black points in panels (C-H) indicate the data. The vertical segments in panel (C-J) indicate 95% credible intervals. In panels (I-J), each point corresponds to a

specific week and age group. The vertical dotted black segments in panels (C-E) indicate the 95% confidence interval around the proportions.

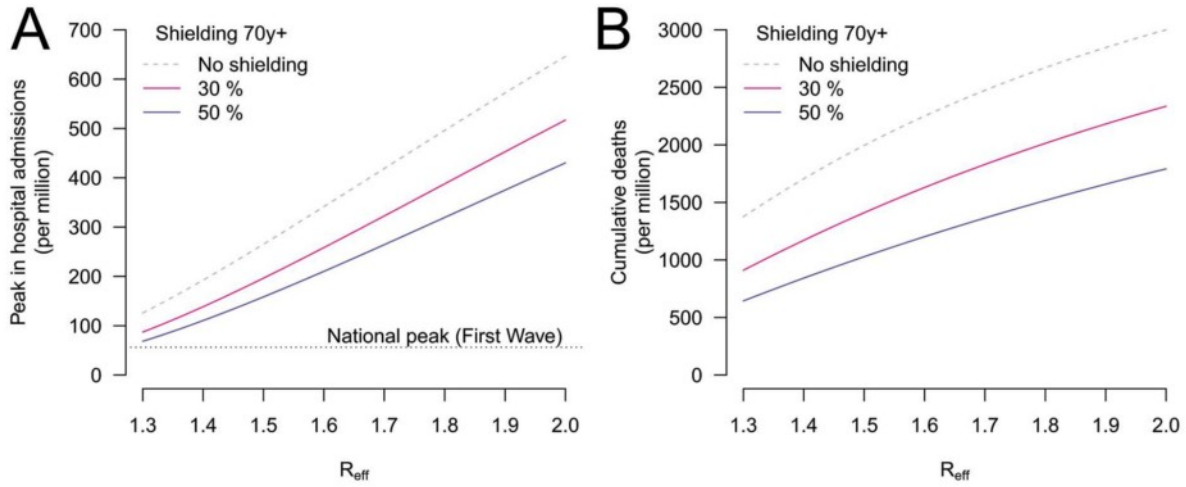

Figure 3: Impact of strategies shielding the elderly population. (A) Peak in hospital admissions per million and **(B)** number of deaths per million as a function of the effective reproduction number R_{eff} assuming a reduction of 50% or 30% in effective contacts of those older than 70 y.o. The number of deaths is computed from the time interventions are implemented until the end of the simulation.

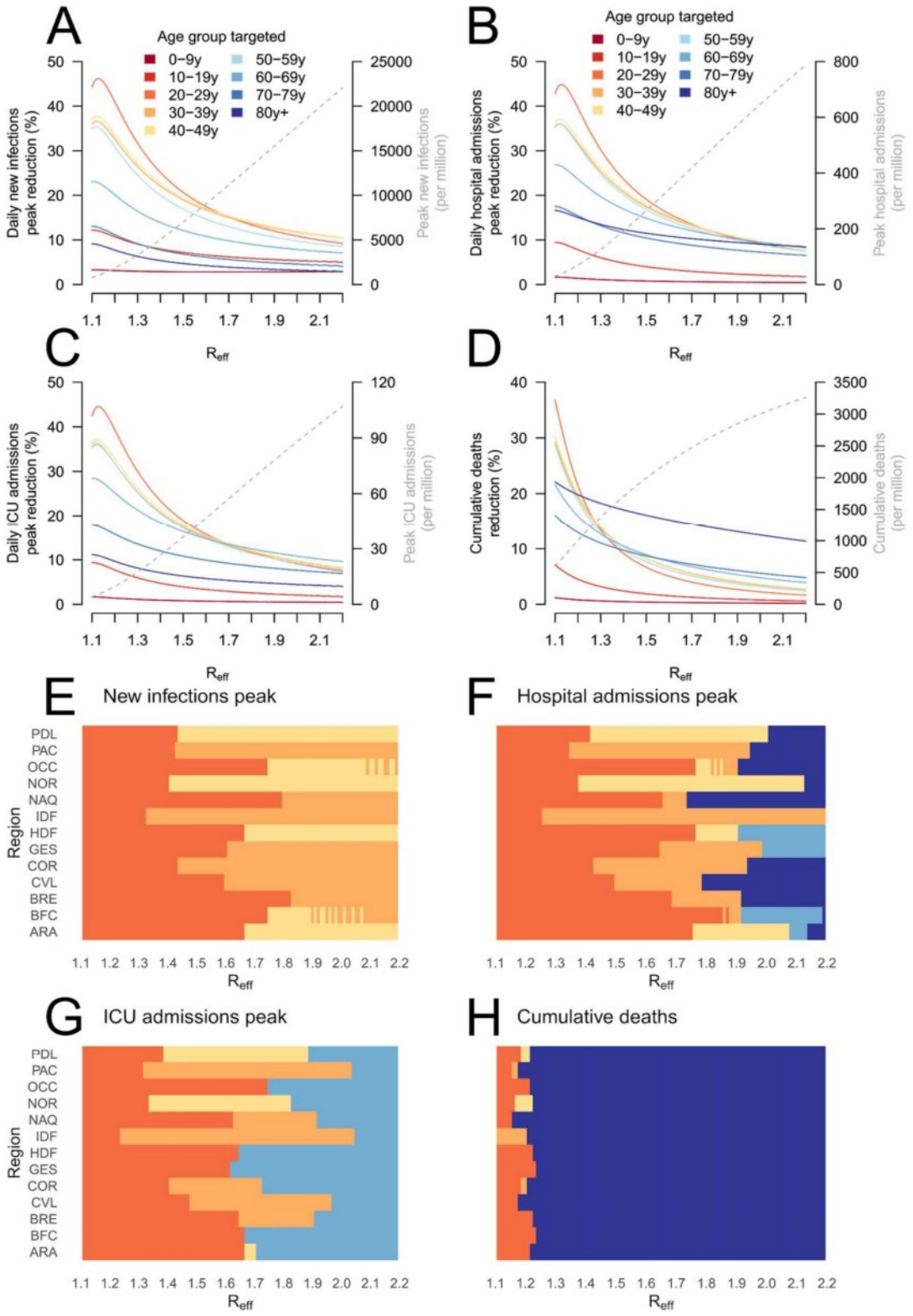
A
Age group targeted
0–9y
10–19y
20–29y
30–39y
40–49y
50–59y
60–69y
70–79y
80y+
Daily new infections peak reduction (%)
Peak new infections (per million)
B
Daily hospital admissions peak reduction (%)
Peak hospital admissions (per million)
C
Daily ICU admissions peak reduction (%)
Peak ICU admissions (per million)
D
Cumulative deaths reduction (%)
Cumulative deaths (per million)
Reff
E
New infections peak
F
Hospital admissions peak
G
ICU admissions peak
H
Cumulative deaths
Region
PDL
PAC
OCC
NOR
NAQ
IDF
HDF
GES
COR
CVL
BRE
BFC
ARA

Figure 4: Impact of strategies targeting specific age groups. Reduction in **(A)** the peak in daily new infections, **(B)** the peak in hospital admissions, **(C)** the peak in daily ICU admissions, **(D)** the number of deaths when individuals in the target age group reduce their effective contacts by 1, as a function of the effective reproduction number R_{eff}, in the Auvergne-Rhône-Alpes region. The grey dotted lines indicate, in the absence of additional measure, the value of the epidemiological metrics. Age-groups for which a reduction of 1 contact results in the highest impact on the reduction of **(E)** the peak in daily new infections, **(F)** the peak in hospital admissions, **(G)** the peak in daily ICU admissions, **(H)** the number of deaths as a function of the effective reproduction number R_{eff}. The number of deaths is computed from the time interventions are implemented until the end of the simulation. Region's abbreviations are detailed in supplementary text.

References

1. H. Salje, C. Tran Kiem, N. Lefrancq, N. Courtejoie, P. Bosetti, J. Paireau, A. Andronico, N. Hozé, J. Richet, C.-L. Dubost, Y. Le Strat, J. Lessler, D. Levy-Bruhl, A. Fontanet, L. Opatowski, P.-Y. Boelle, S. Cauchemez, Estimating the burden of SARS-CoV-2 in France. *Science*. **369**, 208–211 (2020).

2. S. Flaxman, S. Mishra, A. Gandy, H. J. T. Unwin, T. A. Mellan, H. Coupland, C. Whittaker, H. Zhu, T. Berah, J. W. Eaton, M. Monod, Imperial College COVID-19 Response Team, A. C. Ghani, C. A. Donnelly, S. Riley, M. A. C. Vollmer, N. M. Ferguson, L. C. Okell, S. Bhatt, Estimating the effects of non-pharmaceutical interventions on COVID-19 in Europe. *Nature*. **584**, 257–261 (2020).

3. Great Barrington Declaration, (available at https://gbdeclaration.org/).

4. M. A. Miller, C. Viboud, D. R. Olson, R. F. Grais, M. A. Rabaa, L. Simonsen, Prioritization of influenza pandemic vaccination to minimize years of life lost. *J. Infect. Dis.* **198**, 305–311 (2008).

5. J. Wallinga, M. van Boven, M. Lipsitch, Optimizing infectious disease interventions during an emerging epidemic. *Proc. Natl. Acad. Sci. U. S. A.* **107**, 923–928 (2010).

6. I. M. Longini, M. E. Halloran, A. Nizam, M. Wolff, P. M. Mendelman, P. E. Fast, R. B. Belshe, Estimation of the efficacy of live, attenuated influenza vaccine from a two-year, multi-center vaccine trial: implications for influenza epidemic control. *Vaccine*. **18**, 1902–1909 (2000).

7. P. A. Piedra, M. J. Gaglani, C. A. Kozinetz, G. Herschler, M. Riggs, M. Griffith, C. Fewlass, M. Watts, C. Hessel, J. Cordova, W. P. Glezen, Herd immunity in adults against influenza-related illnesses with use of the trivalent-live attenuated influenza vaccine (CAIV-T) in children. *Vaccine*. **23**, 1540–1548 (2005).

8. T. A. Reichert, N. Sugaya, D. S. Fedson, W. P. Glezen, L. Simonsen, M. Tashiro, The Japanese experience with vaccinating schoolchildren against influenza. *N. Engl. J. Med.* **344**, 889–896 (2001).

9. A. S. Monto, F. M. Davenport, J. A. Napier, T. Francis Jr, Effect of vaccination of a school-age population upon the course of an A2-Hong Kong influenza epidemic. *Bull. World Health Organ.* **41**, 537–542 (1969).

10. P. Bosetti, B.-T. Huynh, A. Y. Abdou, M. Sanchez, C. Eisenhauer, N. Courtejoie, J. Accardo, H. Salje, D. Guillemot, M. Moslonka-Lefebvre, P.-Y. Boëlle, G. Béraud, S. Cauchemez, L. Opatowski, Lockdown impact on age-specific contact patterns and behaviours in France (2020), , doi:10.1101/2020.10.07.20205104.

11. E. Goldstein, M. Lipsitch, M. Cevik, On the effect of age on the transmission of SARS-CoV-2 in households, schools and the community. *medRxiv* (2020), doi:10.1101/2020.07.19.20157362.

12. R. M. Viner, O. T. Mytton, C. Bonell, G. J. Melendez-Torres, J. Ward, L. Hudson, C. Waddington, J. Thomas, S. Russell, F. van der Klis, A. Koirala, S. Ladhani, J. Panovska-Griffiths, N. G. Davies, R. Booy, R. M. Eggo, Susceptibility to SARS-CoV-2 Infection Among Children and Adolescents Compared With Adults: A Systematic Review and Meta-analysis. *JAMA Pediatr.* (2020), doi:10.1001/jamapediatrics.2020.4573.

13. Santé Publique France, “COVID-19 : point épidémiologique du 15 octobre 2020” (Santé Publique France, 2020), (available at https://www.santepubliquefrance.fr/maladies-et-traumatismes/maladies-et-infections-respiratoires/infection-a-coronavirus/documents/bulletin-national/covid-19-point-epidemiologique-du-15-octobre-2020).

14. Santé Publique France, “COVID-19 : point épidémiologique du 22 octobre 2020” (Santé Publique France, 2020), (available at https://www.santepubliquefrance.fr/maladies-et-traumatismes/maladies-et-infections-respiratoires/infection-a-coronavirus/documents/bulletin-national/covid-19-point-epidemiologique-du-22-octobre-2020).

15. Santé Publique France, “COVID-19 : point épidémiologique du 29 octobre 2020” (Santé Publique France, 2020), (available at https://www.santepubliquefrance.fr/maladies-et-traumatismes/maladies-et-infections-respiratoires/infection-a-coronavirus/documents/bulletin-national/covid-19-point-epidemiologique-du-29-octobre-2020).

16. A. M. Oster, E. Caruso, J. DeVies, K. P. Hartnett, T. K. Boehmer, Transmission Dynamics by Age Group in COVID-19 Hotspot Counties - United States, April-September 2020. *MMWR Morb. Mortal. Wkly. Rep.* **69**, 1494–1496 (2020).

17. A. M. Clarfield, A. Jotkowitz, Age, ageing, ageism and “age-itation” in the Age of COVID-19: rights and obligations relating to older persons in Israel as observed through the lens of medical ethics. *Isr. J. Health Policy Res.* **9**, 64 (2020).

18. M. Piccoli, T. Tannou, I. Hernandorena, S. Koeberle, [Ethical approach to the issue of confinement of the elderly in the context of the COVID-19 pandemic: Prevention of frailty versus risk of vulnerability]. *Ethics Med Public Health*. **14**, 100539 (2020).

19. T. L. Beauchamp, J. F. Childress, *Principles of biomedical ethics. 5th ed* ({Oxford University Press}, 2021).

20. G. Béraud, S. Kazmercziak, P. Beutels, D. Levy-Bruhl, X. Lenne, N. Mielcarek, Y. Yazdanpanah, P.-Y. Boëlle, N. Hens, B. Dervaux, The French Connection: The First Large Population-Based Contact Survey in France Relevant for the Spread of Infectious Diseases. *PLoS One*. **10**, e0133203 (2015).

21. N. Lefrancq, J. Paireau, N. Hozé, N. Courtejoie, Y. Yazdanpanah, L. Bouadma, P.-Y. Boëlle, F. Chereau, H. Salje, S. Cauchemez, Evolution of outcomes for patients hospitalized during the first SARS-CoV-2 pandemic wave in France. *HAL* (2020),

(available at https://hal.archives-ouvertes.fr/hal-02946545).

22. O. Diekmann, J. A. Heesterbeek, J. A. Metz, On the definition and the computation of the basic reproduction ratio R0 in models for infectious diseases in heterogeneous populations. *J. Math. Biol.* **28**, 365–382 (1990).

23. B. Visseaux, C. Burdet, G. Voiriot, F.-X. Lescure, T. Chougar, O. Brugière, B. Crestani, E. Casalino, C. Charpentier, D. Descamps, J.-F. Timsit, Y. Yazdanpanah, N. Houhou-Fidouh, Prevalence of respiratory viruses among adults, by season, age, respiratory tract region and type of medical unit in Paris, France, from 2011 to 2016. *PLoS One*. **12**, e0180888 (2017).

24. Insee − Institut national de la statistique et des études économiques, (available at https://www.insee.fr/).

25. J. Chevalier, G. de Pouvourville, Valuing EQ-5D using time trade-off in France. *Eur. J. Health Econ.* **14**, 57–66 (2013).

26. F. Sandmann, N. Davies, A. Vassall, W. John Edmunds, M. Jit, Centre for the Mathematical Modelling of Infectious Diseases COVID-19 working group, The potential health and economic value of SARS-CoV-2 vaccination alongside physical distancing in the UK: transmission model-based future scenario analysis and economic evaluation, , doi:10.1101/2020.09.24.20200857.

27. A. J. van Hoek, A. Underwood, M. Jit, E. Miller, W. J. Edmunds, The impact of pandemic influenza H1N1 on health-related quality of life: a prospective population-based study. *PLoS One*. **6**, e17030 (2011).

28. M. Baguelin, A. Camacho, S. Flasche, W. John Edmunds, Extending the elderly- and risk-group programme of vaccination against seasonal influenza in England and Wales: a cost-effectiveness study. *BMC Medicine*. **13** (2015), , doi:10.1186/s12916-015-0452-y.

29. B. H. Cuthbertson, S. Roughton, D. Jenkinson, G. Maclennan, L. Vale, Quality of life in the five years after intensive care: a cohort study. *Crit. Care*. **14**, R6 (2010).

30. J. Griffiths, R. A. Hatch, J. Bishop, K. Morgan, C. Jenkinson, B. H. Cuthbertson, S. J. Brett, An exploration of social and economic outcome and associated health-related quality of life after critical illness in general intensive care unit survivors: a 12-month follow-up study. *Critical Care*. **17** (2013), p. R100.

31. N. G. Davies, CMMID COVID-19 working group, P. Klepac, Y. Liu, K. Prem, M. Jit, R. M. Eggo, Age-dependent effects in the transmission and control of COVID-19 epidemics. *Nature Medicine*. **26** (2020), pp. 1205–1211.

Acknowledgments

Funding: We acknowledge financial support from the Investissement d'Avenir program, the Laboratoire d'Excellence Integrative Biology of Emerging Infectious Diseases program (grant ANR-10-LABX-62-IBEID), Santé Publique France, the INCEPTION project (PIA/ANR-16-CONV-0005), the European Union's Horizon 2020 research and innovation program under grant 101003589 (RECOVER), AXA and Institut Pasteur.

Author contributions: CTK and SC conceived the study. CTK, PB, JP, PC, HS, NL and LO performed the analyses. CTK and SC wrote the first draft. All authors contributed to revisions of the manuscript.

Competing interests: None declared

Supplementary materials

Materials and methods

Supplementary text

Figures S1 to S24

Tables S1 to S9

Materials and Methods

Hospitalization data

We use hospitalization data extracted from the SI-VIC database. This database is maintained by the ANS (Agence du Numérique en Santé) and provides real time information on the COVID-19 patients hospitalized in public and private French hospitals. Data, including age, hospitalization date, outcome and region, are sent daily to Santé Publique France, the French national public health agency. All COVID-19 cases are either biologically confirmed or present with a computed tomographic image highly suggestive of SARS-CoV-2 infection. Missing ages are imputed assuming that the age distribution of newly hospitalized patients for a given week in a given region is similar to the age distribution obtained from patients with age information. We restrict our analysis to patients hospitalized in general ward beds (*Hospitalisation conventionnelle*) or ICU beds (*Hospitalisation réanimatoire: réanimation, soins intensifs et unité de surveillance continue*) and discard patients that are hospitalized in emergency care units (*Soins d'urgence*), psychiatric care (*Hospitalisation psychiatrique*) or long-term and rehabilitation care (*Soins de suite et réadaptation*). We consider events (hospitalizations, transfers, deaths or discharges) by date of occurrence and correct observed data for reporting delays (*1*).

Test data

SIDEP (Système d'Information de Dépistage Populationnel - Information system for population-based testing) is a national surveillance system describing RT-PCR and antigen tests results for SARS-CoV-2 arising from all private and public French laboratories. For the time window used in this analysis, antigen tests were not included in the database. Anonymized data are transmitted daily to Santé Publique France, the French national public health agency, through a secured platform. Upon testing, individuals are asked to report whether they are experiencing symptoms. Test results are reported by date of nasopharyngeal swab and include patient information such as age, delay since symptoms onset and postal code of the home address. When the home address is not available, the postal code of the lab performing testing is indicated. In case of multiple swabs for a single patient, if test results are both positive and negative, the first test with positive results is kept. If all test results are negative, the results of the first test are kept. The number of tests reported in the SIDEP surveillance system for metropolitan France increased throughout summer from 208,214 on the week of 15 June 2020 to 1,115,644 on the week of 14 September 2020 (Figure S23).

Social contact data

We extracted social contact information from SocialCov, an online survey where participants aged >18 y.o. are invited to describe the contacts they had during the previous day. In the survey, a contact was defined as either a physical contact (e.g. a kiss or a handshake), or a close contact (e.g. face to face conversation at less than 1 meter). Collected information includes the age of the person involved in the contact and the setting where the contact happened (i.e. work, home, leisure place, or others). In addition, respondents living with one or more minors were asked to provide the same information for one of them. The survey was advertised following the same approach as in (*10*). Data were collected in accordance with the regulation in force in France for the protection and security of personal data. The answers of 1295 participants were collected between 30 July and 27 September 2020. To comply with the constraints in the survey design of the COMES-F study (*20*), used here as the reference for the mixing patterns in France, individuals with more than 40 contacts were excluded from this analysis, reducing the population from an initial number of 1628 to 1550 (including the underaged population). For each age-group 0-9 y.o., 10-19 y.o., 20-29 y.o., 30-39 y.o., 40-49 y.o., 50-59 y.o., 60-69 y.o., 70-79 y.o., and >80 y.o., we computed the mean daily number of contacts, see Table S2 and Figure S22.

Transmission model

To describe the dynamics of SARS-CoV-2 in the French population and the trajectories of hospitalized patients, we use an age-stratified deterministic compartmental model whose structure follows the one described in Salje et al (*1*). In short, infectiousness begins on average 4 days after infection. On average 5 days after infection, infected individuals move to the I compartment. Symptoms onset occurs upon entry into the I compartment for some of the infected individuals. A subset of infected individuals will develop a severe form of the disease and eventually be hospitalized. The probability of hospitalization upon infection is age-dependent, as estimated in Salje et al (*1*). The model is stratified in $n_{age} = 9$ age groups: 0-9 y.o., 10-19 y.o., 20-29 y.o., 30-39 y.o., 40-49 y.o., 50-59 y.o., 60-69 y.o., 70-79 y.o., and >80 y.o.

Estimating the age-specific probability of ICU admission given hospitalization and probability of death given hospitalization

During the first pandemic wave of SARS-CoV-2 in Metropolitan France, we estimated that the mean probability of ICU admission given hospitalization decreased from 27% to 14% (*1*). The probability of death given hospitalization also decreased through time since the

beginning of the SARS-CoV-2 pandemic in France (*21*). To capture the latest modifications of these probabilities, we adjust the age-specific probabilities of ICU admission given hospitalization and probabilities of death given hospitalization estimated in Salje et al (*1*) accounting for the most recent changes. We estimate the relative change in the probability of ICU admission given hospital admission and death given hospitalization among individuals aged 0-39 y.o., 40-49 y.o., 50-59 y.o., 60-69 y.o., 70-79 y.o. and over 80 y.o. using an approach described elsewhere (*21*). In short, we use a linelist of patients hospitalized in general wards and ICU beds extracted from the SI-VIC database and derive changes in age-specific outcome probabilities (*e.g.* ICU admissions, deaths) for the following time periods: T1: 13 March 2020 - 10 May 2020 ; T2: 11 May 2020 - 12 July 2020 ; T3: 13 July 2020 - 30 September 2020 (Table S3, S4) For these, we compute the probabilities of ICU admission and death given hospitalization for the following age-groups: 0-19 y.o., 20-29 y.o., 30-39 y.o., 40-49 y.o., 50-59 y.o., 60-69 y.o., 70-79 y.o. and over 80 y.o. (Table S5). Using this approach, we are also able to estimate the proportion of death that occurs in ICUs for each of these 3 time-periods (Table S6).

Changes in transmission intensity and contact patterns

Assumptions about contact patterns before 11 May 2020 (i.e. the end of the country-wide lockdown) are similar to the ones used in Salje et al (*1*). The contact matrix describing mixing patterns before the implementation of a country-wide lockdown on 17 March 2020 are extracted from the COMES-F survey (*20*). During the lockdown, the contact matrix was modified to account for the strict measures put in place. We assume a new change in the reproduction number and in contact patterns on 11 May 2020, when restrictive measures started to be progressively lifted. We also assume another change in transmission on a date that depends on the region (Table S7), in line with the observed increase in the proportion of positive tests at the regional level (Figure 1). For these two post-lockdown time periods, we estimate reproduction numbers ($R_{postLock}$ and $R_{rebound}$) for each region. At the national level, this corresponds to a reproduction number of 2.90 before 17 March 2020 that was subsequently reduced to 0.67 during the lockdown (*1*).

Modelling contact patterns between the different age-groups

Let ${c_{i,j}}^{baseline}$ denote the mean daily number of contacts that an individual aged i had with an individual aged j in the pre-lockdown period. These values are extracted from the COMES-F survey (*20*). Let α_i denote the reduction of contacts for individuals aged i during a time-period of interest To ensure that the total number of contacts between individuals aged i and individuals aged j is equal to the total number of contacts between

individuals aged j and individuals aged i in the population, we assume that the reduction of contacts between age groups i and j is equal to $\beta_{i,j} = min\,(\alpha_i, \alpha_j)$. The mean daily number of contacts that an individual aged i has with individuals aged j is thus equal to $\beta_{i,j} \cdot {c_{i,j}}^{baseline}$. As we are working with normalized contact matrices (i.e. contact matrices divided by their maximum eigenvalue), we are only interested in the relative reduction between different age-groups. We thus set: $\alpha_{20-29} = 1$ and do not constrain the other α_i values to be lower than 1.

We assume that contact patterns changed at two distinct periods: first, with the progressive easing of control measures after 11 May 2020 and second at the time of the epidemic rebound (Table S7). We estimate parameters related to the reduction of contacts for age-groups: 0-9 y.o.;10-19 y.o.; 30-39 y.o.; 40-49 y.o.; 50-59 y.o.; 60-69 y.o.;70-79 y.o.; and over 80 y.o. for each of the two time-periods. We assume that parameters describing the change in mixing patterns from the easing of the lockdown until the rebound are the same in all regions and that mixing patterns during the rebound are region-specific.

Computing the proportion of positive symptomatic tests by age-group from the model

To reduce the impact of potential changes in testing policies, we calibrate our model on the proportion of positive tests amongst symptomatic individuals being tested. Let $S_+(t,a)$ and $S_-(t,a)$ denote respectively the number of positive and negative tests among symptomatic individuals of age a being tested at time t. We assume that $S_-(t,a)$ is constant over time. Let $p(a)$ denote the probability of being symptomatic upon SARS-CoV-2 infection amongst individuals aged a. Let $N(a)$ denote the number of individuals aged a. Let $I(t,a)$ denote the number of individuals aged a in compartment I (i.e. the compartment in which a subset of infectious individuals develops symptoms) predicted by the model. The proportion of positive tests among symptomatic individuals of age a that were tested is:

$$P_+(t,a) = \frac{S_+(t,a)}{S_+(t,a) + S_-(t,a)} = \frac{p(a) \cdot I(t,a)}{p(a) \cdot I(t,a) + S_-(t,a)} = \frac{\gamma_a \cdot I(t,a)/N(a)}{\gamma_a \cdot I(t,a)/N(a) + 1}$$

where $\gamma_a = p(a)/S_-(t,a) \cdot N(a)$ is a parameter to be estimated. $S_-(t,a)/N(a)$ is the prevalence of symptoms suggestive of COVID-19 that cannot be attributed to a SARS-CoV-2 infection in individuals aged a at time t. We assume that γ_a is constant across age-groups and regions and use the notation γ to refer to this quantity. Furthermore, we assume a three days delay between symptoms onset and testing, in line with the reported delay between symptoms onset and date of test (Figure S24).

Computing the effective reproduction number in an age-structured population

The basic reproduction number R_0 corresponds to the average number of infections resulting from a single index case in a completely susceptible population. The effective reproduction number R_{eff} accounts for the fact that a fraction of the population is immuned and no longer contributes to the disease spread. To compute the effective reproduction number, we use the next-generation matrix approach (*22*). Let ${p_S}^i(t)$ denote the proportion of the population aged i susceptible to infection at time *t*. Let β denote the transmission rate and D the average duration of the infectious period. Let $c_{i,j}$ denote the mean daily number of contacts that and individual aged i has with someone aged j.

The effective reproduction number is then derived as:

$R_{eff}(t) = \beta \cdot D \cdot \rho(\ [c_{i,j} \cdot {p_S}^j(t)]_{ij}\ )$ where $\rho(M)$denotes the spectral radius of a matrix M.

Time window used for the model calibration

The SIDEP system was initiated on 13 May 2020 with a progressive increase in the number of laboratories reporting the results (from 4562 on the week of 13 May 2020 to 5447 on the week of 15 June 2020) (Figure S25). On the week of 13 May 2020, 17.2% of individuals with a positive test result (without missing information about the presence/absence of symptoms) reported developing symptoms more than 2 weeks prior to the test. From the week of 15 June 2020, this proportion was down to 1.0%. From the week of 15 June 2020, the number of laboratories reporting results in the SIDEP database remains quite stable. From this date, the proportion of tested individuals with a delay between symptoms onset and test greater than 2 weeks also remained constant (Figure S24). We thus begin the calibration of our model on test data on the week of 15 June 2020. We fitted our model to the proportion of positive tests among symptomatic individuals as this quantity is most likely less sensitive to contact tracing efficiency in a period where the circulation of other respiratory viruses remains low (*23*).

Following the increase in the number of positive tests and hospital admissions, control measures have progressively been implemented in some regions, resulting in a decrease in the reproduction number (e.g. Provence-Alpes Côte d'Azur region). As we aim to describe transmission patterns during summer before the implementation of additional measures, we define region-specific final date of calibration (the latest possible date being 27 September 2020) based on the time-trends of the proportion of positive tests among symptomatic individuals (Table S8).

The age distribution of hospital admissions predicted by our model depends on our assumptions about mixing patterns. Due to the delay between infection and hospital admissions, individuals admitted to hospital during the two weeks following lockdown release will have mostly been infected during the lockdown period. As we fix the contact matrix describing age-specific contact patterns during the lockdown, we only begin the calibration of our model on age-stratified data on 25 May 2020 (i.e. 2 weeks after the end of the country-wide lockdown). Between 11 May 2020 and 24 May 2020, we calibrate our model on the daily number of hospital admissions occurring in each metropolitan French region.

Models are calibrated using SI-VIC data (extracted from the SI-VIC database on 12 October 2020) between 11 May 2020 and the region-specific final date of calibration and on the weekly proportion of positive tests among individuals reporting symptoms (extracted from SIDEP data) between 15 June 2020 and the region-specific final date of calibration.

Statistical framework

Parameters are estimated using a Bayesian Markov Chain Monte Carlo framework. We develop a Metropolis-Hastings algorithm with lognormal proposals and uniform priors for all the parameters. Chains are run with 15,000 iterations removing 3,000 iterations of burn-in.

Let ${Adm_{hosp}}^{obs}(t)$ and ${Adm_{hosp}}^{pred}(t)$ denote the observed and expected number of COVID-19 hospital admissions on day t for the whole population. After 24 May 2020, age-groups are specifically considered and data are aggregated at the week level. Let ${Adm_{hosp}}^{obs}(w,a)$ and ${Adm_{hosp}}^{pred}(w,a)$ denote the observed and predicted number of COVID-19 patients belonging to age group a admitted to hospital on week w. Let $X^{obs}(w,a)$ and $N^{obs}(w,a)$denote the number of positive tests and the number of tests amongst symptomatic individuals being tested on week w in age-group a. Let ${P_+}^{pred}(w,a)$ denote the proportion of positive tests amongst symptomatic individuals tested predicted by the model for age group a on week w. The likelihood function until day T is then defined as:

$$L_T = L^{hosp}(T) \cdot \mathrm{L}^{\mathrm{Age-Hosp}}(T) \cdot L^{\mathrm{Age-Test}}(T)$$

with:

$$L^{hosp}(T) = \prod_{t=11\,May}^{24\,May} g({Adm_{hosp}}^{obs}(t) | {Adm_{hosp}}^{pred}(t))$$

$$\mathrm{L}^{\mathrm{Age-Hosp}}(T) = \prod_{w=w_1}^{w_T} \prod_{a=1}^{n_{age}} g(Adm_{hosp}{}^{obs}(w,a) |\, Adm_{hosp}{}^{pred}(w,a))$$

$$L^{Age-Tests}(T) = \prod_{w=w_2}^{w_T} \prod_{a=1}^{n_{age}} h(X^{obs}(w,a) |\, N^{obs}(w,a), P_+{}^{pred}(w,a))$$

Where $w_1$corresponds to the week starting on 25 May 2020, w_T corresponds to the week of time T, $w_2$corresponds to the first week for which we consider test data to be reliable (15 June 2020), $g(\cdot\,|X)$ is a Poisson distribution of mean X and $h(\cdot \mid N,p)$is the density of a binomial distribution $B(N,p)$. n_{age} corresponds to the number of age groups in the model.

Estimating contact rates between age-groups from the modified matrices

Contact patterns before the lockdown are described by the matrix $C^{baseline} = [c_{i,j}{}^{baseline}]_{i,j}$, with $(i,j) \in \{1,\ldots,n_{age}\}^2$ depicting the contacts between the different age groups, extracted from the COMES-F survey. (*20*)

We estimate contact patterns as well as the reproduction number for the time period that follows the lockdown. Let $C^{rebound}$denote the contact matrix estimated for the rebound period. In line with the notations used above, we have:

$$C^{rebound} = (c_{i,j}{}^{rebound}) \;=\; (min(\alpha_i{}^{rebound}, \alpha_j{}^{rebound}) \cdot c_{i,j}{}^{baseline})$$

Numerous factors, including changing climate conditions, more outdoor activities or the adoption of protective behaviours such as masks or hand hygiene, can have an impact on the transmission risk associated with a contact with an infected individual (i.e. the transmission rate). We fix the value of the mean daily number of contacts of individuals aged 20-29 y.o. to the one reported in the SocialCov survey during summer. Let $\mu^{SocialCov}$denote the mean daily number of contacts of individuals aged 20-29 y.o. reported in the SocialCov survey (*10*). We then estimate the mean daily number of contacts that an individual aged i has with individuals aged j during the rebound period $c_{i,j}{}^{eff}$by:

$$c_{i,j}{}^{eff} = \frac{\mu^{SocialCov}}{\sum_j c_{20-\quad,j}{}^{rebound}} \cdot c_{i,j}{}^{rebound}$$

This also enables us to derive the transmission rate during the rebound period by:

$$\beta^{rebound} = \frac{R^{rebound}}{D \cdot \rho(C^{eff})}$$

Simulation of intervention strategies targeting single age-groups

We run forward simulations to evaluate the impact of social distancing strategies that reduce contacts in targeted age-groups, starting from the region-specific date of end of calibration. We assume that when an individual reduces his/her contacts, such a reduction is homogeneously distributed across contacts with the different age-groups. For a strategy targeting age-groups a corresponding to a reduction of x contacts, we define a new contact matrix as:

$C^{interv} = ({c_{i,j}}^{interv}) = (min({\alpha_i}^{interv}, {\alpha_j}^{interv}) \cdot {c_{i,j}}^{eff})$

With ${\alpha_i}^{interv} = \frac{(\sum_j {c_{a,j}}^{eff}) - x}{(\sum_j {c_{a,j}}^{eff})}$ if $i = a$ and ${\alpha_i}^{interv} = 1$ otherwise.

For each age-group a, we run a range of strategies with reductions of contacts varying between 0 and $\sum_j {c_{a,j}}^{eff}$.

We explore the impact of such intervention strategies on the peak in new infections, the peak in hospital and ICU admissions, the number of deaths arising after the date of change in contact patterns, as well as the life-years lost and QALYs lost after the date where the intervention reducing the number of contacts is implemented. Scenarios are simulated until 18 October 2022.

Computing the number of deaths, years of life lost and quality adjusted years of life lost arising from infections occurring after the date of change in contacts patterns

Based on the age-specific probabilities of death given hospitalization estimated between 13 July 2020 and 30 September 2020 (Table S5), we compute the number of deaths arising from infections occurring after the date of change in contact patterns and the corresponding number of years of life lost until the end of the simulation. Life expectancies for a given age group were computed using data from the National Institute for Statistics and Economic Studies (Institut national de la statistique et des études économiques - INSEE) (*24*). We also compute the quality adjusted years of life lost arising from infections occurring after the date of change in contact patterns. We use age-specific utilities derived for the French setting (*25*). We follow the approach proposed by Sandmann et al. (*26*) to derive the quality-adjusted life years (QALYs) loss per symptomatic cases, non-fatal

hospitalized cases in general wards et non-fatal hospitalized cases admitted in ICUs. We assume that a symptomatic case results in a loss of 0.008 QALYs (*27*), a non-fatal hospitalization in general ward beds in a loss of 0.018 QALYs (*27*, *28*) and a non-fatal ICU hospitalization in a loss of 0.15 QALYs (*29*, *30*). To compute the number of symptomatic infections, we use the age-specific proportion of clinical infections, as estimated in Davies et al (*31*). The corresponding weights used to compute the number of life years lost and quality adjusted life years lost arising from deaths are reported in Table S9.

Supplementary text

The abbreviations used for the names of the metropolitan French regions are:

ARA: Auvergne-Rhônes-Alpes
BFC: Bourgogne-Franche-Comté
BRE: Bretagne
CVL: Centre Val de Loire
COR: Corse
GES: Grand Est
HDF: Hauts-de-France
IDF: Île-de-France
NAQ: Nouvelle-Aquitaine
NOR: Normandie
OCC: Occitanie
PAC: Provence Alpes Côte d'Azur
PDL: Pays de la Loire

Supplementary materials

Figure S1

Figure S1: Map of the 13 regions of metropolitan France

Figure S2

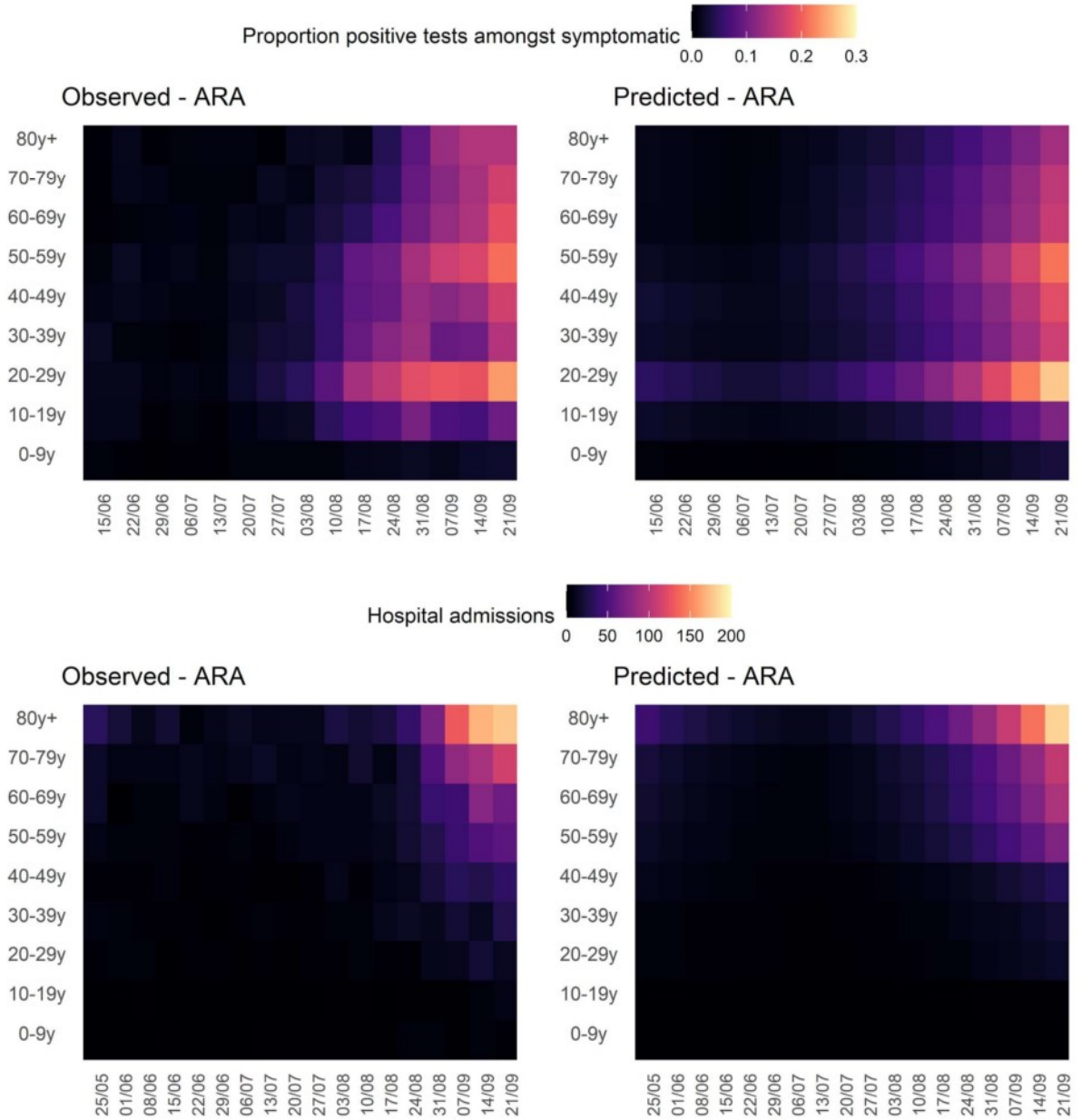

Figure S2: Predicted and observed dynamics of the epidemic in Auvergne-Rhône-Alpes across age-groups. (Top left) Observed and **(Top right)** predicted dynamics of the proportion of positive tests among symptomatic individuals tested by age-group. **(Bottom left)** Observed and **(Bottom right)** predicted dynamics of the weekly hospital admissions by age-group.

Figure S3

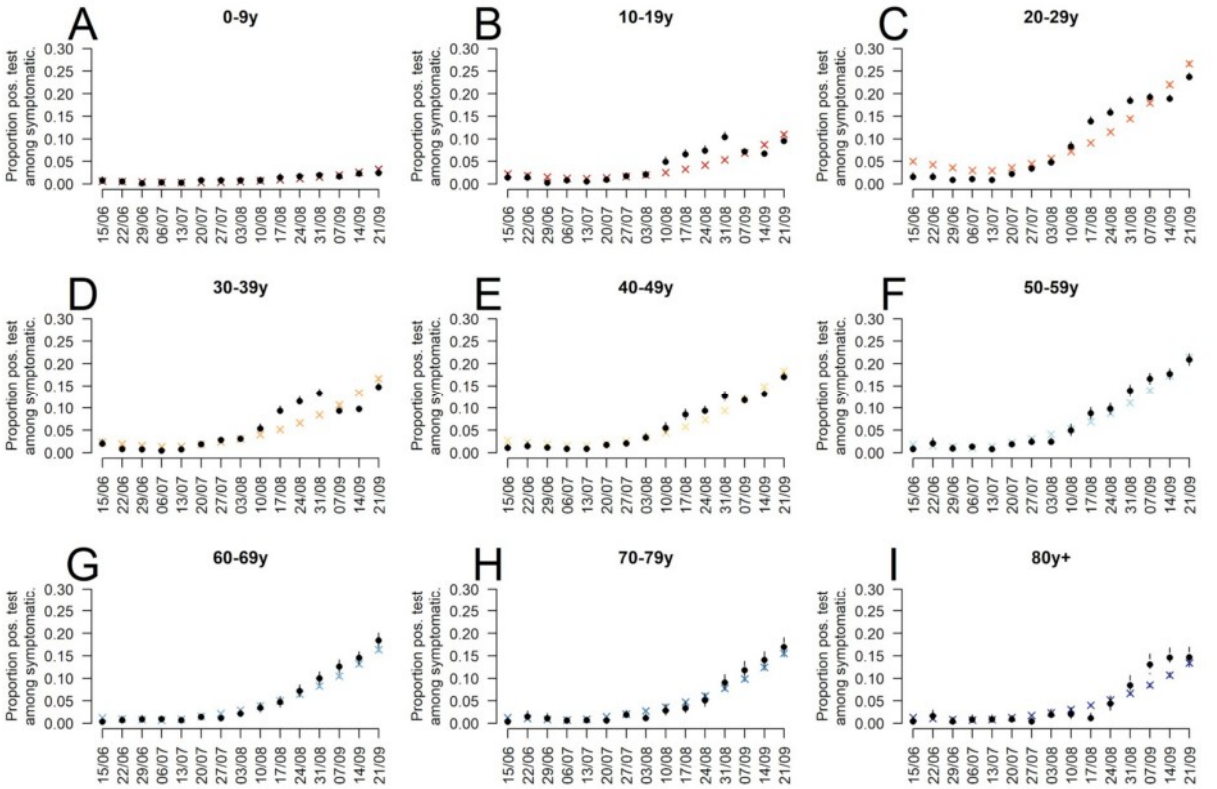

Figure S3: : Model-predicted and observed proportion of positive tests among symptomatic individuals in Auvergne-Rhône-Alpes by age group. Proportion of positive test among symptomatic individuals aged **(A)** 0-9 y.o., **(B)** 10-19 y.o., **(C)** 20-29 y.o., **(D)** 30-39 y.o., **(E)** 40-49 y.o., **(F)** 50-59 y.o., **(G)** 60-69 y.o., **(H)** 70-79 y.o., **(I)** >80 y.o. in Auvergne-Rhône-Alpes. The colored crosses and segments indicate model predictions. The black points with dotted segments indicate the proportions of positive tests among symptomatic individuals extracted from the SIDEP database.

Figure S4

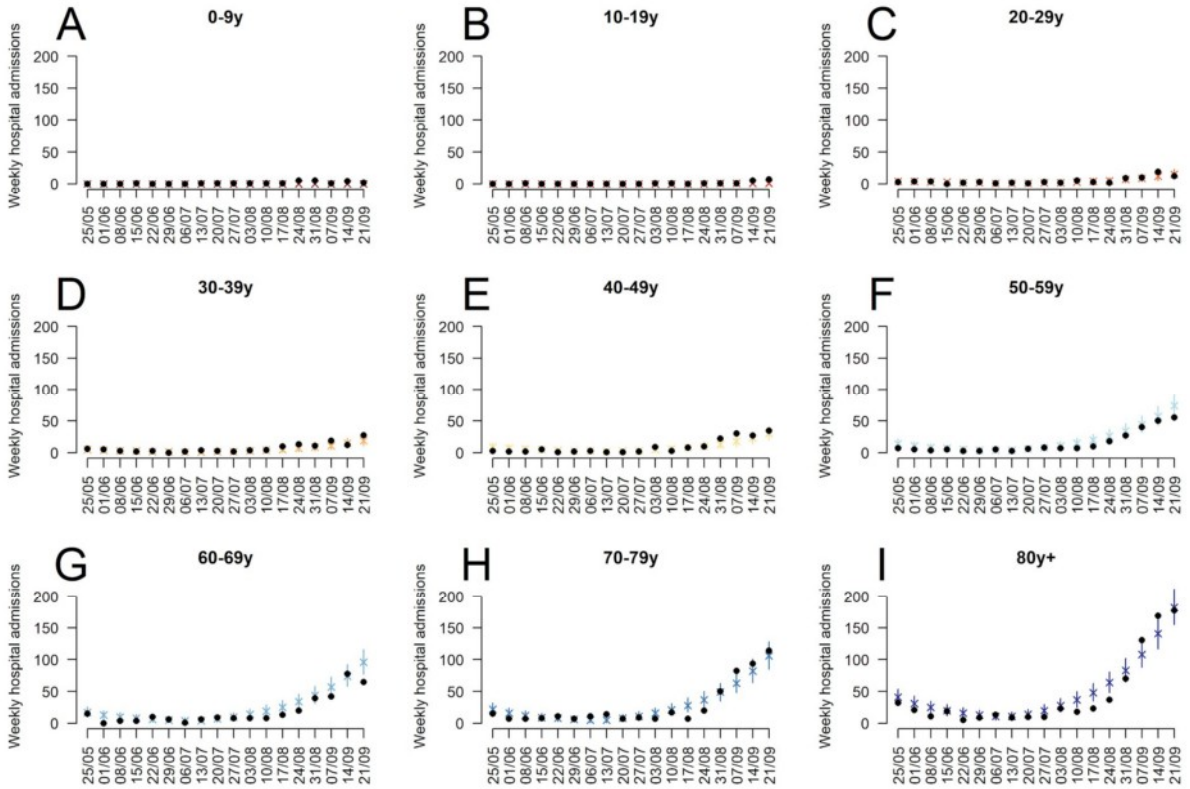

Figure S4: Model predicted and observed age-stratified hospital admissions in Auvergne-Rhône-Alpes by age group. Weekly hospital admissions of individuals aged **(A)** 0-9 y.o., **(B)** 10-19 y.o., **(C)** 20-29 y.o., **(D)** 30-39 y.o., **(E)** 40-49 y.o., **(F)** 50-59 y.o., **(G)** 60-69 y.o., **(H)** 70-79 y.o., **(I)** >80 y.o. in Auvergne-Rhône-Alpes. The colored crosses and segments indicate model predictions. The black points indicate weekly hospital admissions extracted from the SI-VIC database.

Figure S5

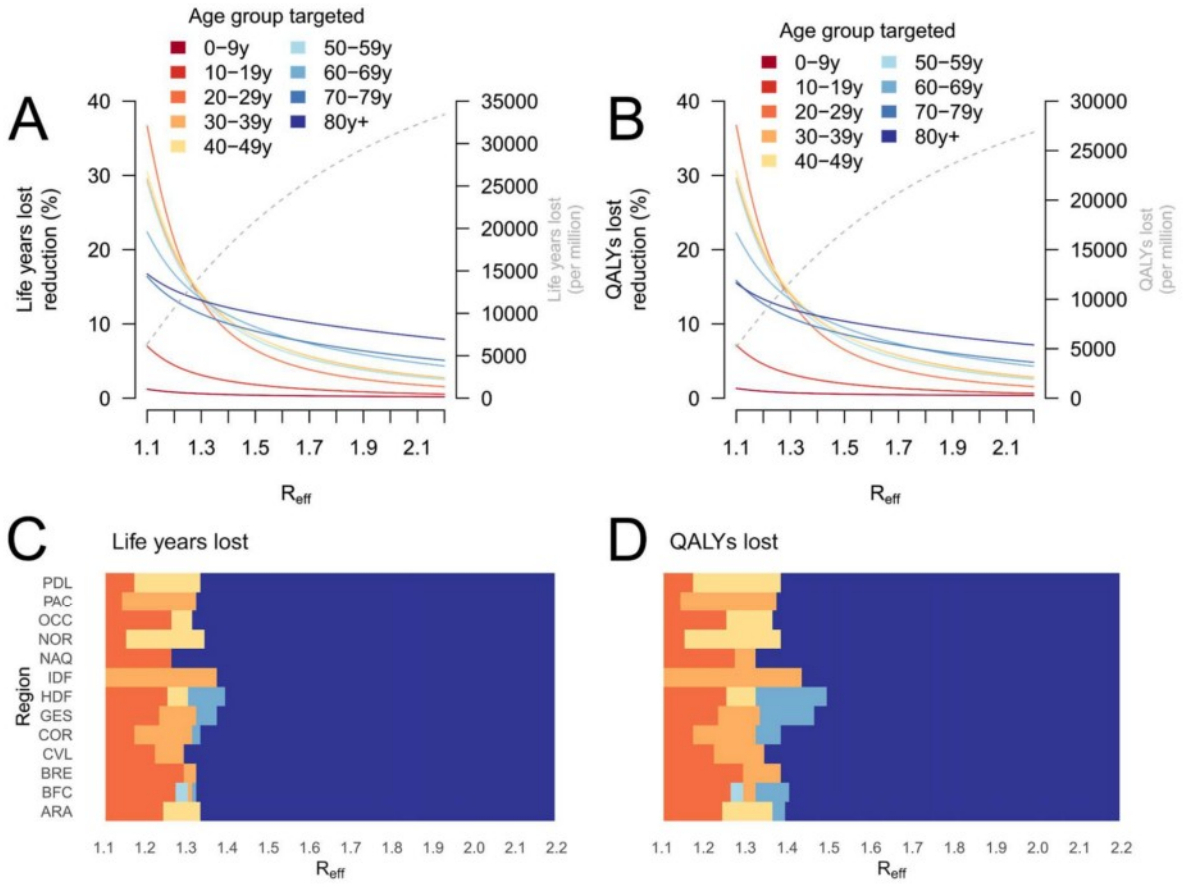

Figure S5: Impact of strategies targeting specific age groups on the number of life-years lost. Reduction in **(A)** the number of life-years lost and **(B)** the number of QALYs lost in Auvergne-Rhône-Alpes region as a function of the effective reproduction number R_{eff} when the intervention is implemented for a reduction of 1 contact. The grey dotted lines indicate, in the absence of additional measure, the value of the target metrics. Age-groups for which a reduction of 1 contact results in the highest impact on the reduction of **(C)** the number of life years lost and **(D)** the number of QALYs lost as a function of the effective reproduction number R_{eff}. Region's abbreviations are detailed in supplementary text.

Figure S6

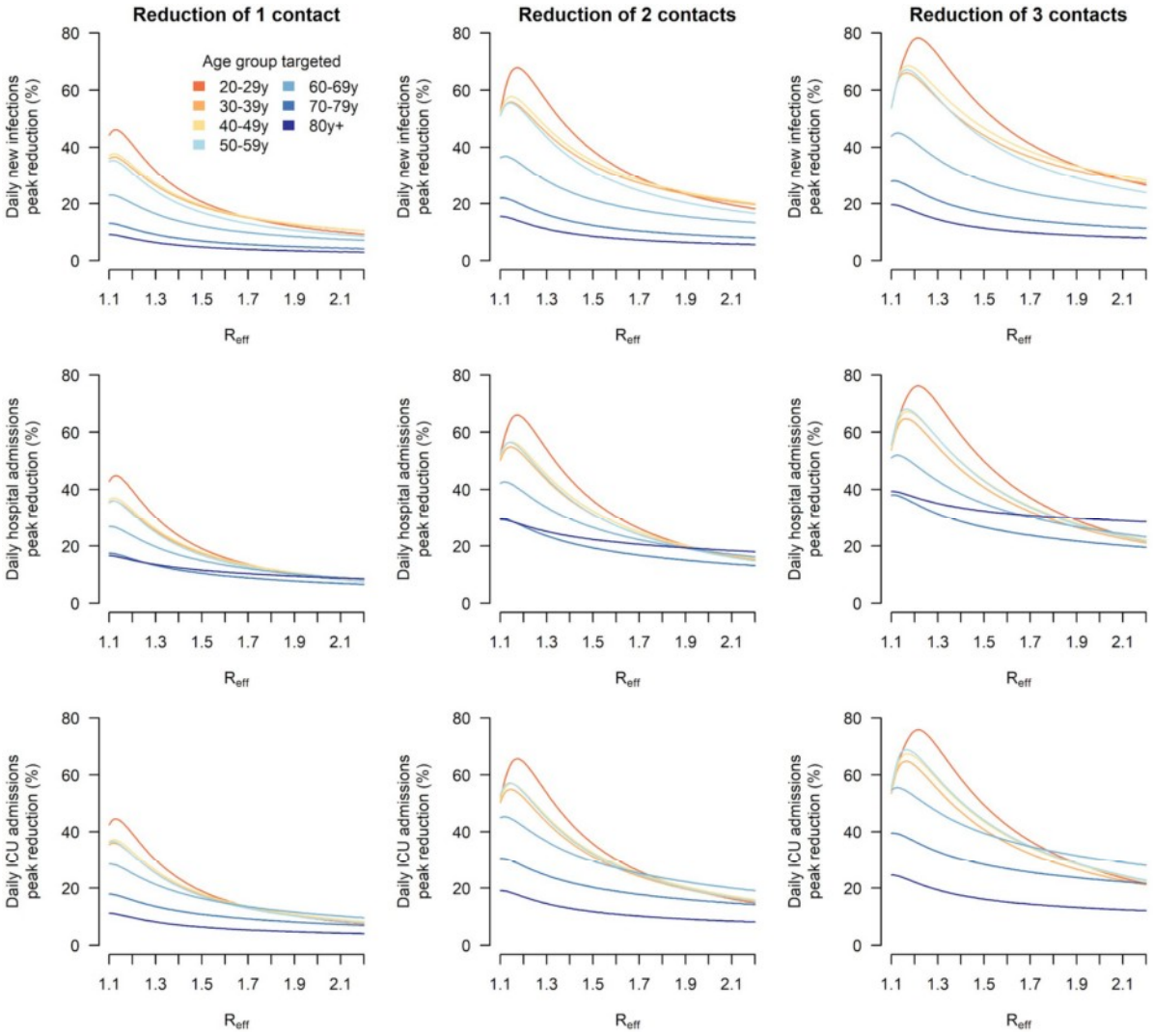

Figure S6: Impact of larger reduction of contacts for strategies targeting different age groups in Auvergne-Rhône-Alpes on the peak in daily new infections (first line), the peak in hospital admissions (second line) and the peak in daily ICU admissions (third line) as a function of the effective reproduction number R_{eff} when the intervention is implemented. Results are displayed for a reduction of 1 contact (first column), 2 contacts (second column) and 3 contacts (third column) in the targeted age groups.

Figure S7

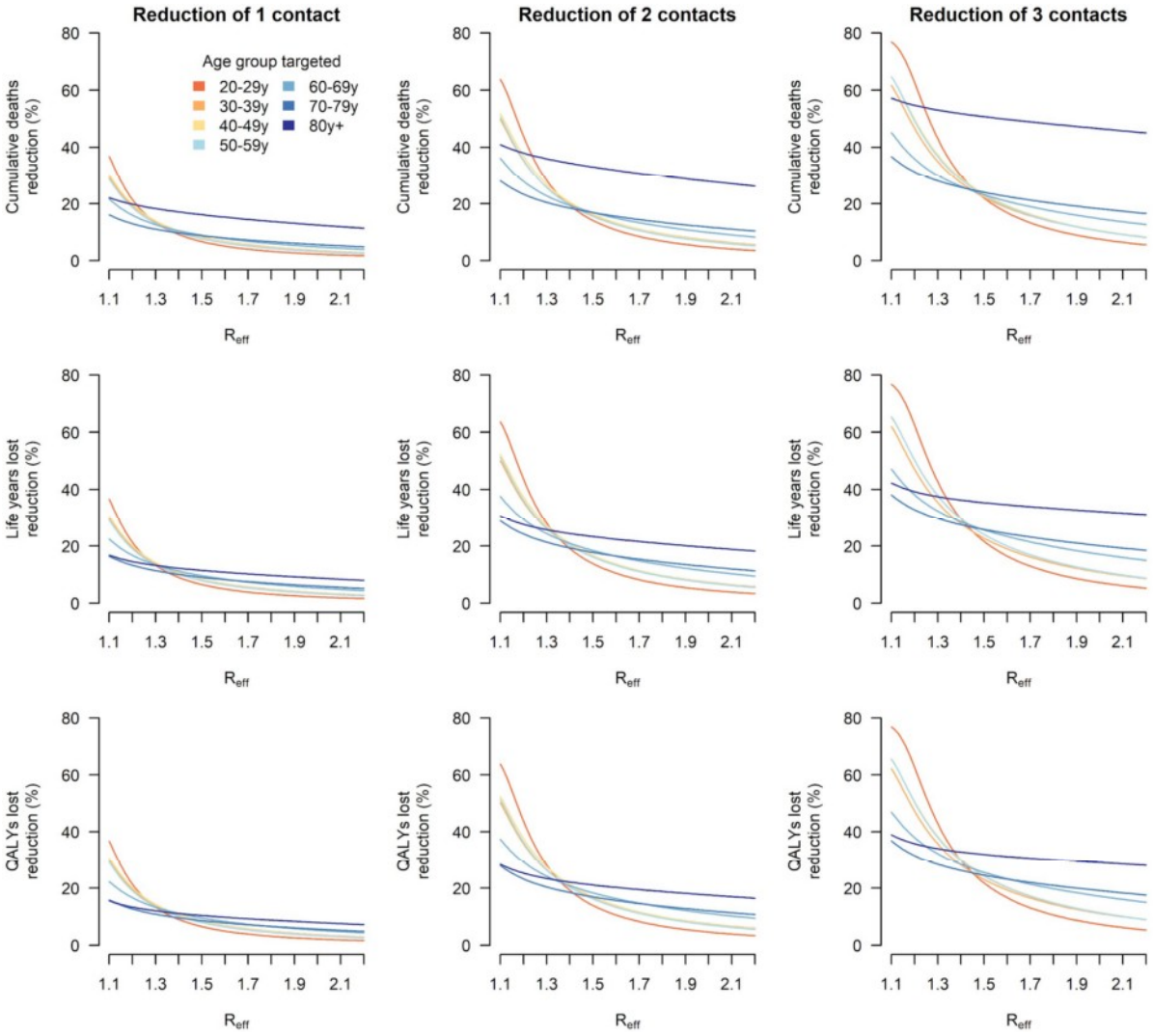

Figure S7: Impact of larger reduction of contacts for strategies targeting different age groups in Auvergne-Rhône-Alpes on the number of deaths (first line), life years lost (second line) and QALYs lost (third line) after the implementation of the intervention as a function of the effective reproduction number R_{eff} when the intervention is implemented.

Figure S8

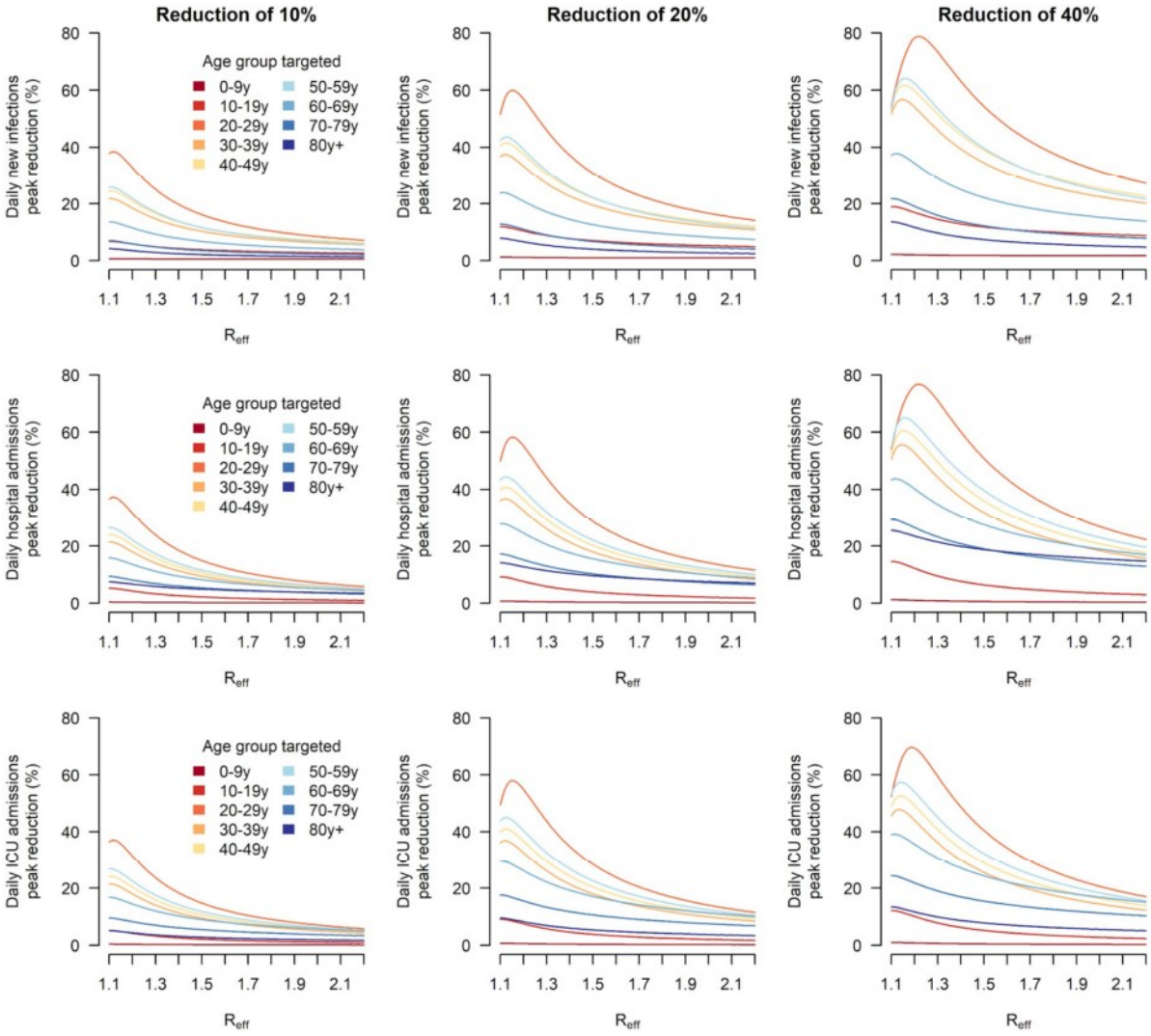

Figure S8: Impact of strategies targeting different age groups in Auvergne-Rhône-Alpes on the peak in daily new infections (first line), the peak in hospital admissions (second line) and the peak in daily ICU admissions (third line) as a function of the effective reproduction number R_{eff} when the intervention is implemented. Results are displayed for a reduction of 10% (first column), 20% (second column) and 40% (third column) in the number of contacts of the targeted age groups.

Figure S9

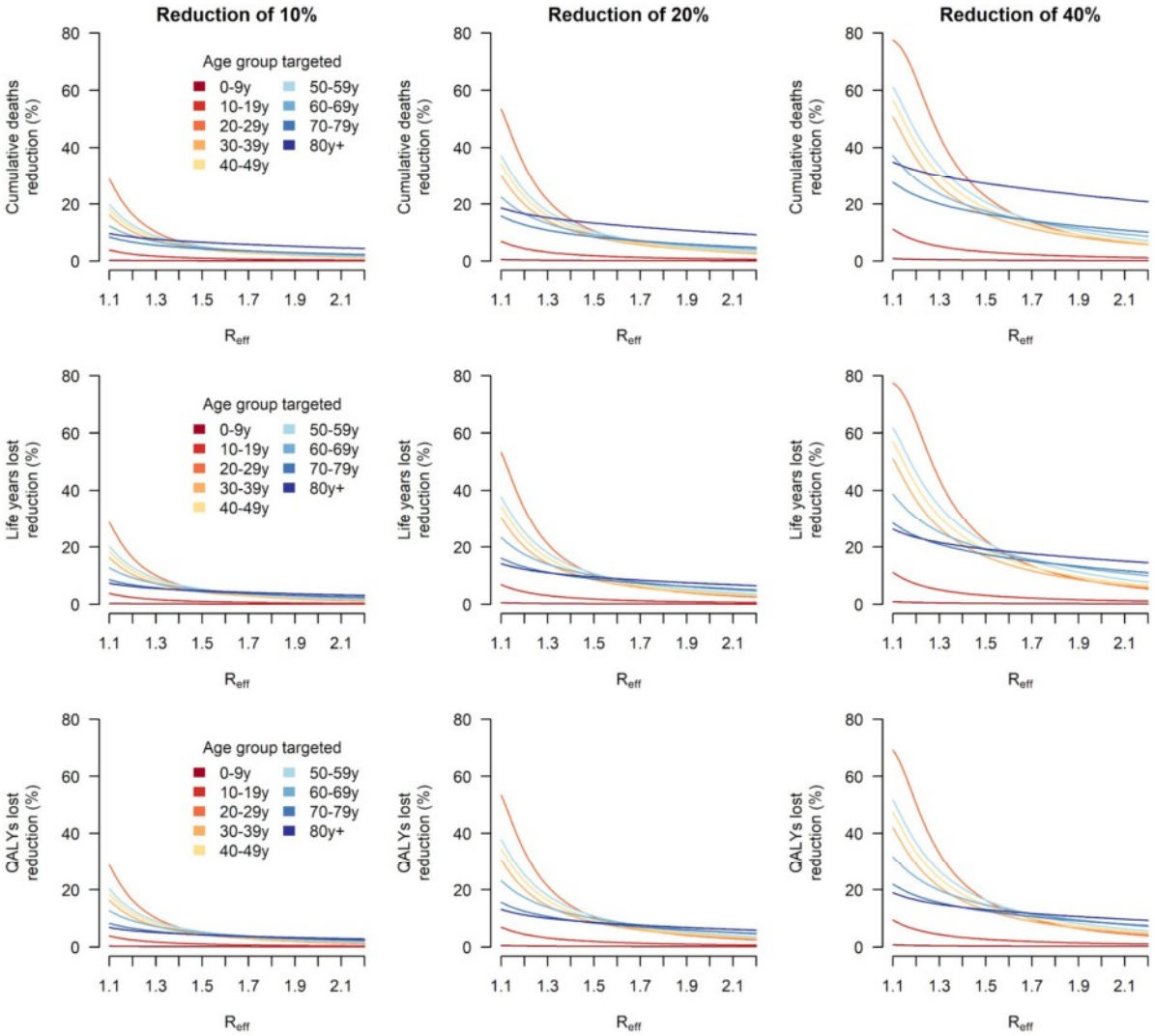

Figure S9: Impact of strategies targeting different age groups in Auvergne-Rhône-Alpes on the number of deaths (first line), the life years lost (second line) and the QALYs lost (third line) as a function of the effective reproduction number R_{eff} when the intervention is implemented. Results are displayed for a reduction of 10% (first column), 20% (second column) and 40% (third column) in the number of contacts of the targeted age groups.

Legend for Figures S10-S21

Proportion of positive test among symptomatic individuals aged **(A)** 0-9 y.o., **(B)** 10-19 y.o., **(C)** 20-29 y.o., **(D)** 30-39 y.o., **(E)** 40-49 y.o., **(F)** 50-59 y.o., **(G)** 60-69 y.o., **(H)** 70-79 y.o., **(I)** >80 y.o. Weekly hospital admissions of individuals aged **(J)** 0-9 y.o., **(K)** 10-19 y.o., **(L)** 20-29 y.o., **(M)** 30-39 y.o., **(N)** 40-49 y.o., **(O)** 50-59 y.o., **(P)** 60-69 y.o., **(Q)** 70-79 y.o., **(R)** >80 y.o. The colored crosses and segments indicate model predictions. The colored crosses and segments indicate model predictions. The black points with dotted segments in panels (A-I) indicate the proportions of positive tests among symptomatic individuals extracted from the SIDEP database. The black points in panels (J-R) indicate weekly hospital admissions extracted from the SI-VIC database.

Figure S10: Model predictions and observations in Bourgogne-Franche-Comté

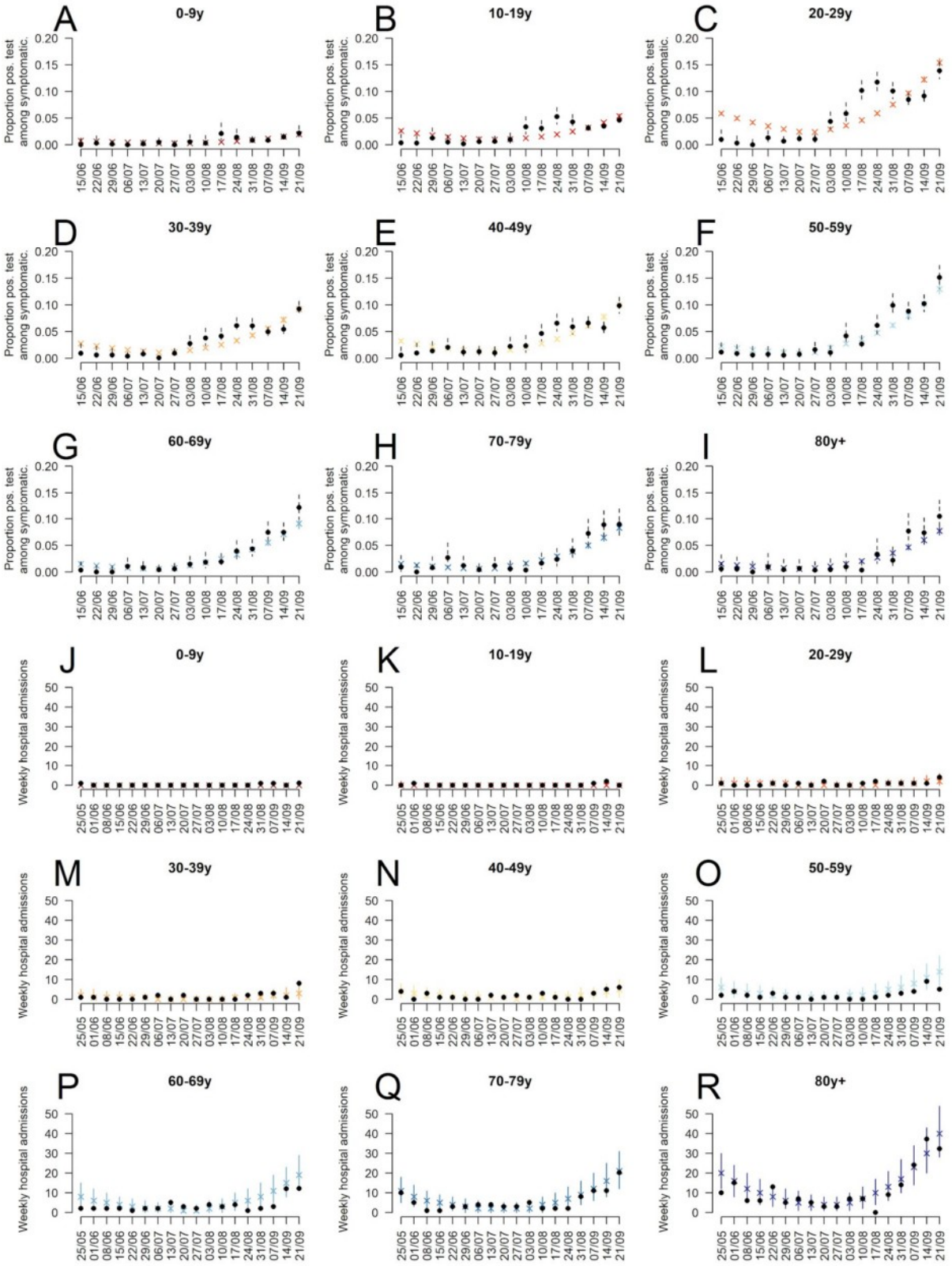

Figure S11: Model predictions and observations in the Bretagne region

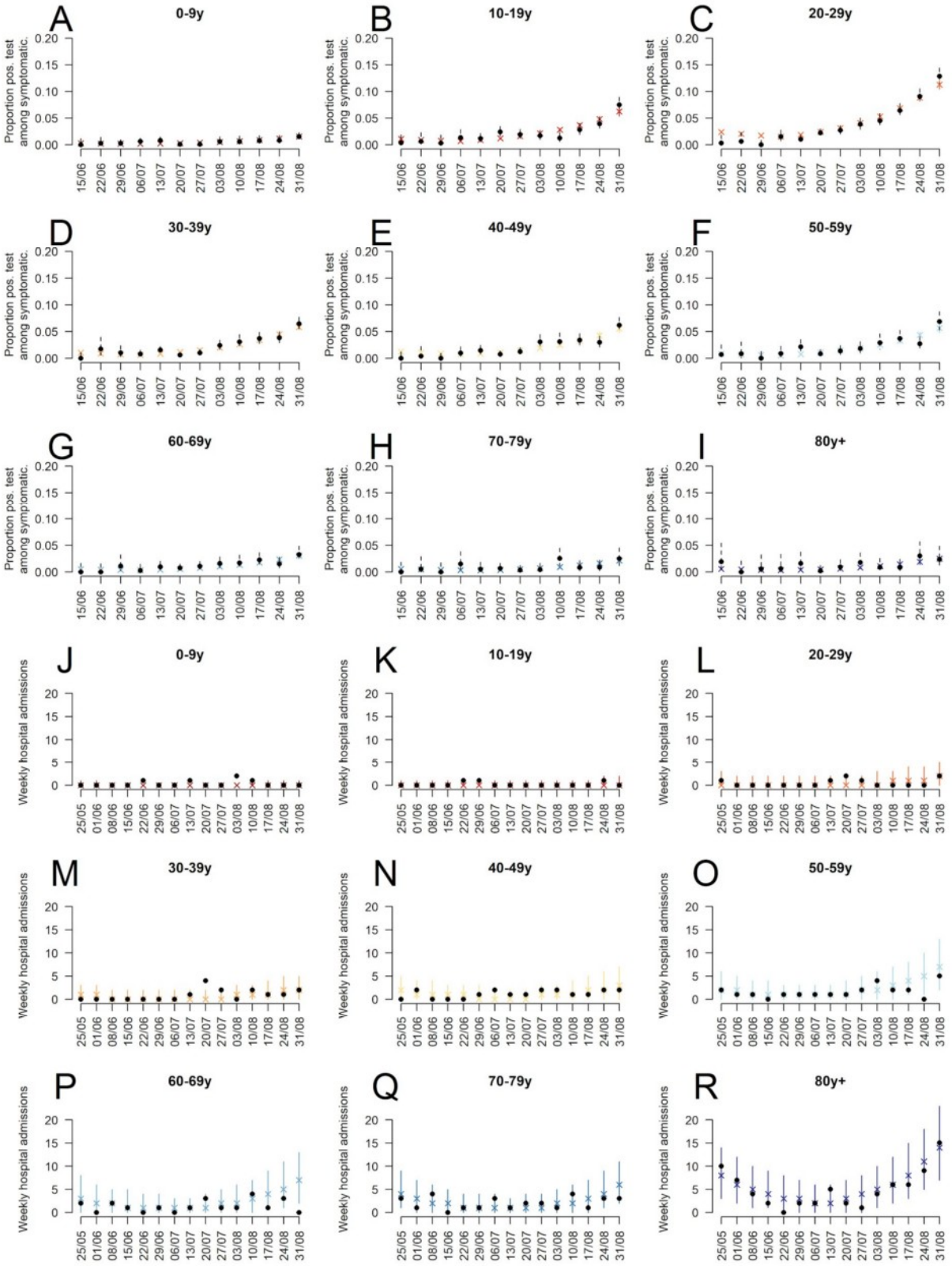

Figure S12: Model predictions and observations in the Centre-Val de Loire region

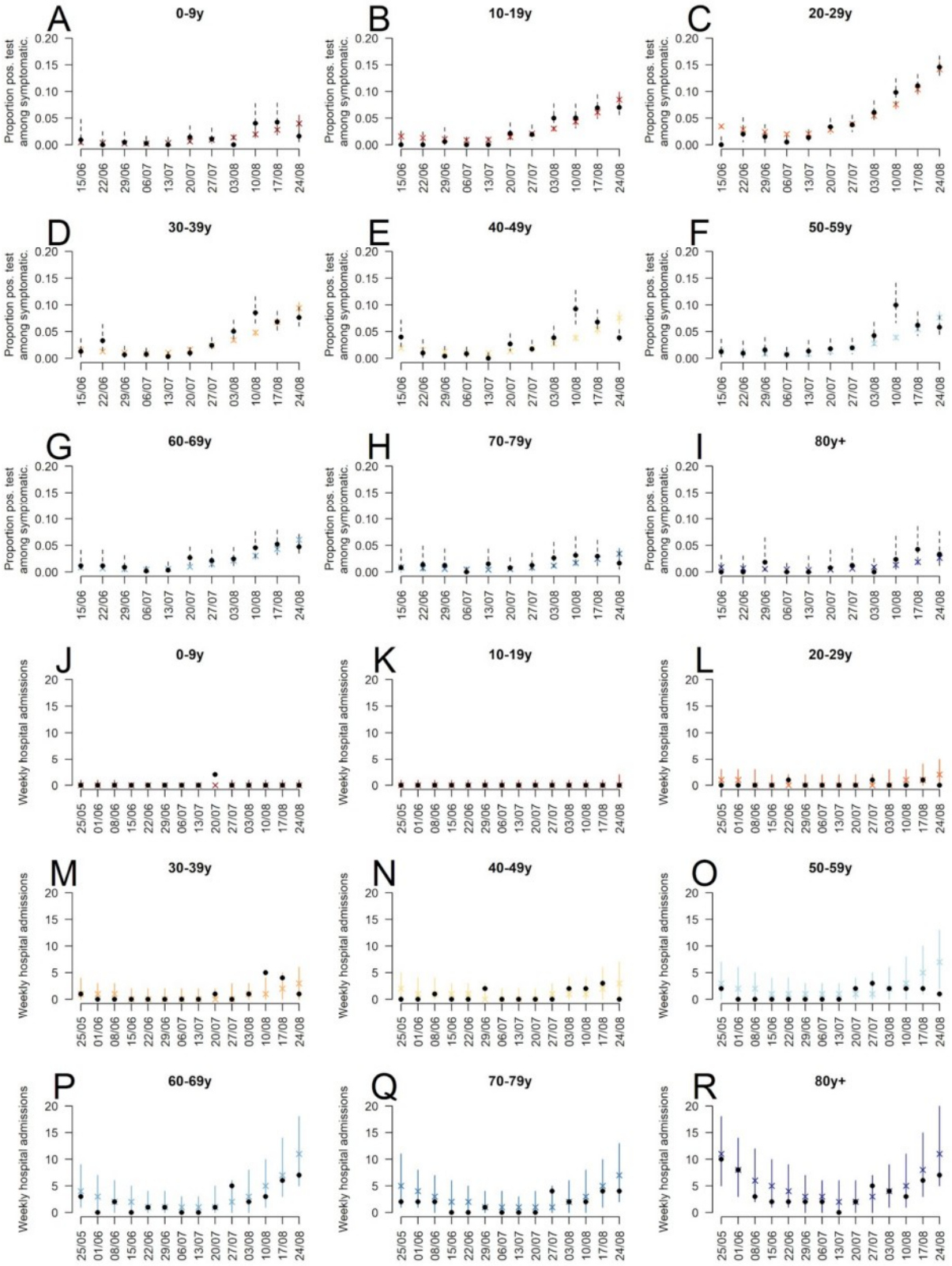

Figure S13: Model predictions and observations in the Corse region

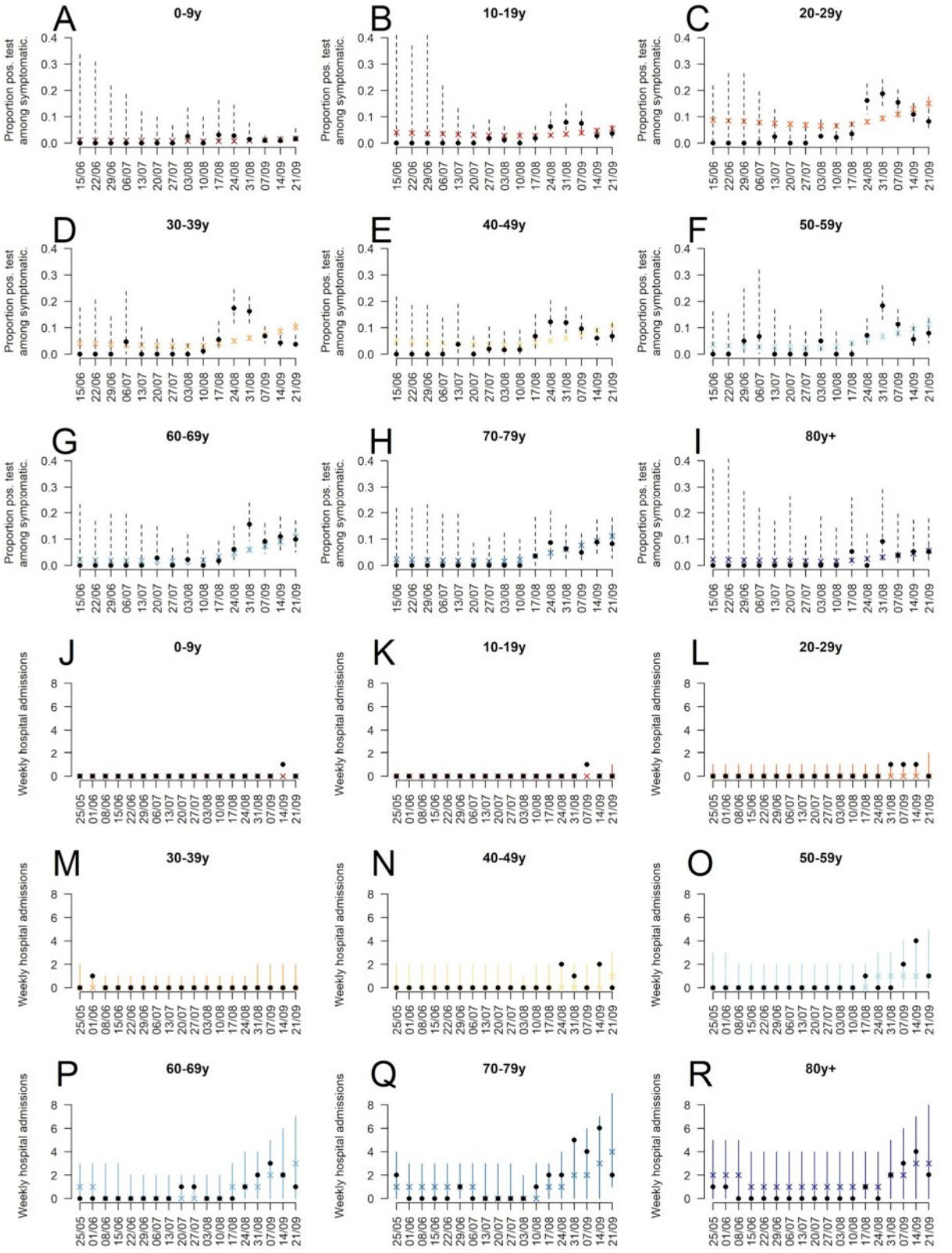

Figure S14: Model predictions and observations in the Grand Est region

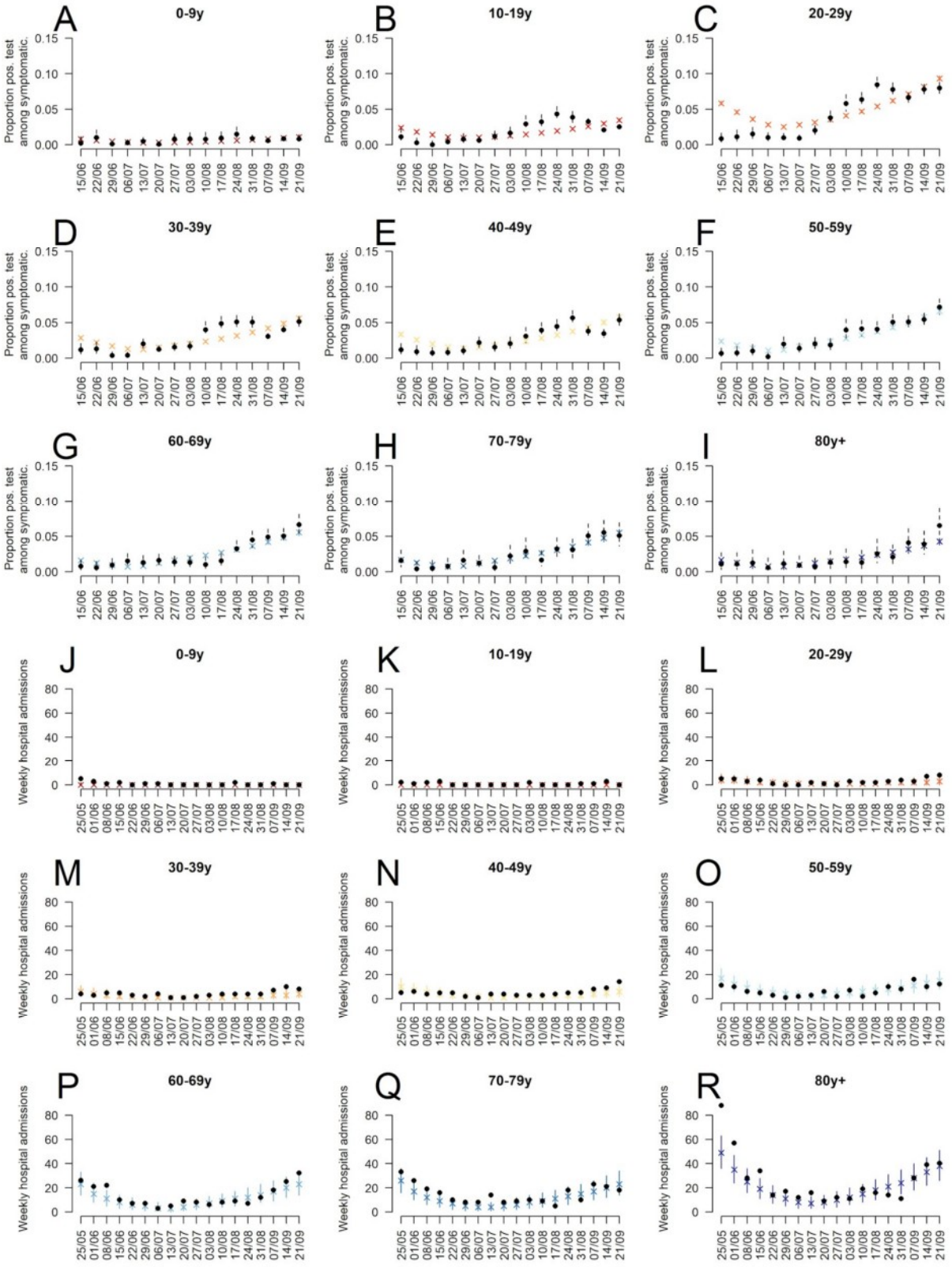

Figure S15: Model predictions and observations in the Hauts-de-France region

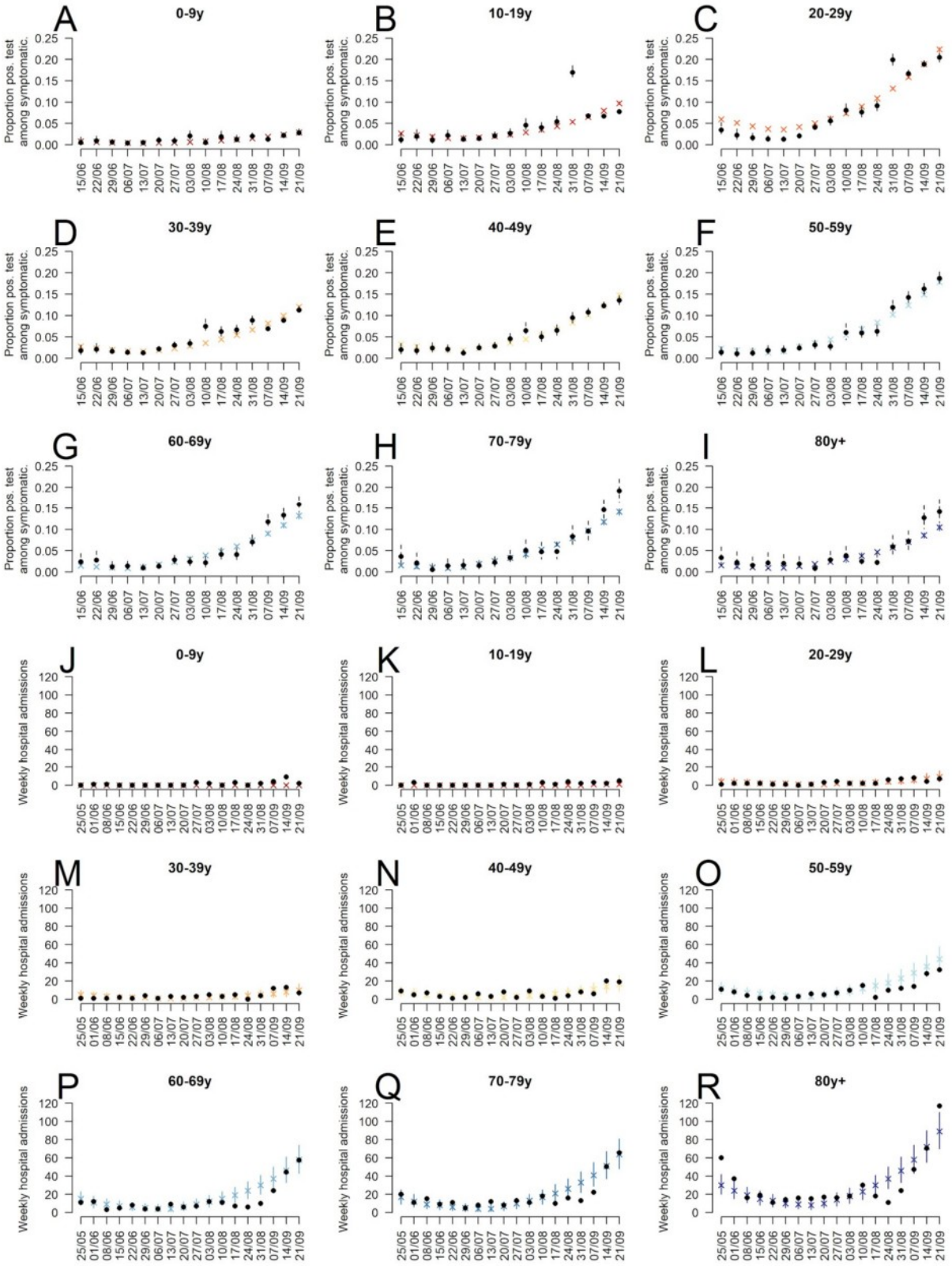

Figure S16: Model predictions and observations in the Île-de-France region

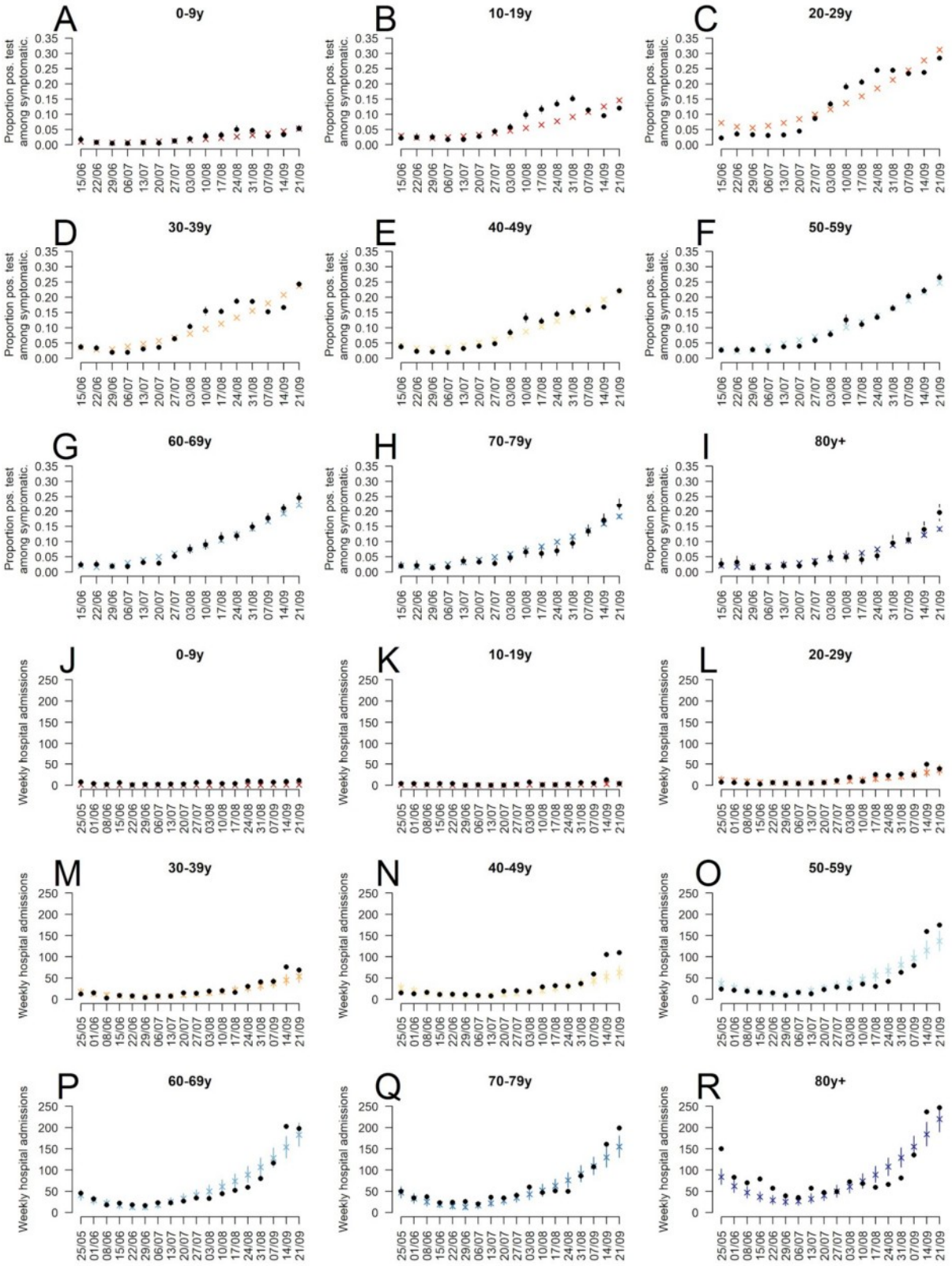

Figure S17: Model predictions and observations in the Nouvelle-Aquitaine region

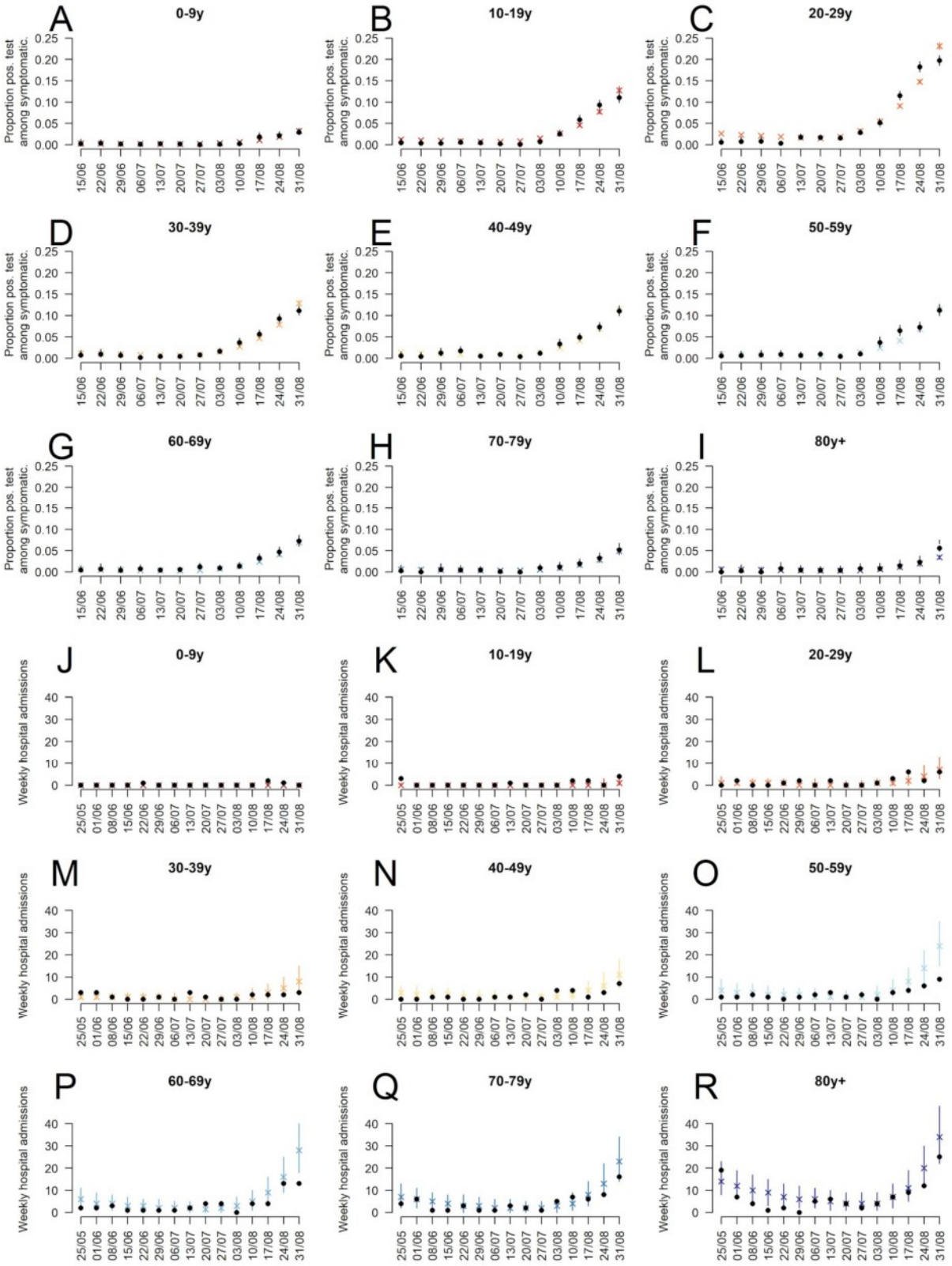

Figure S18: Model predictions and observations in the Normandie region

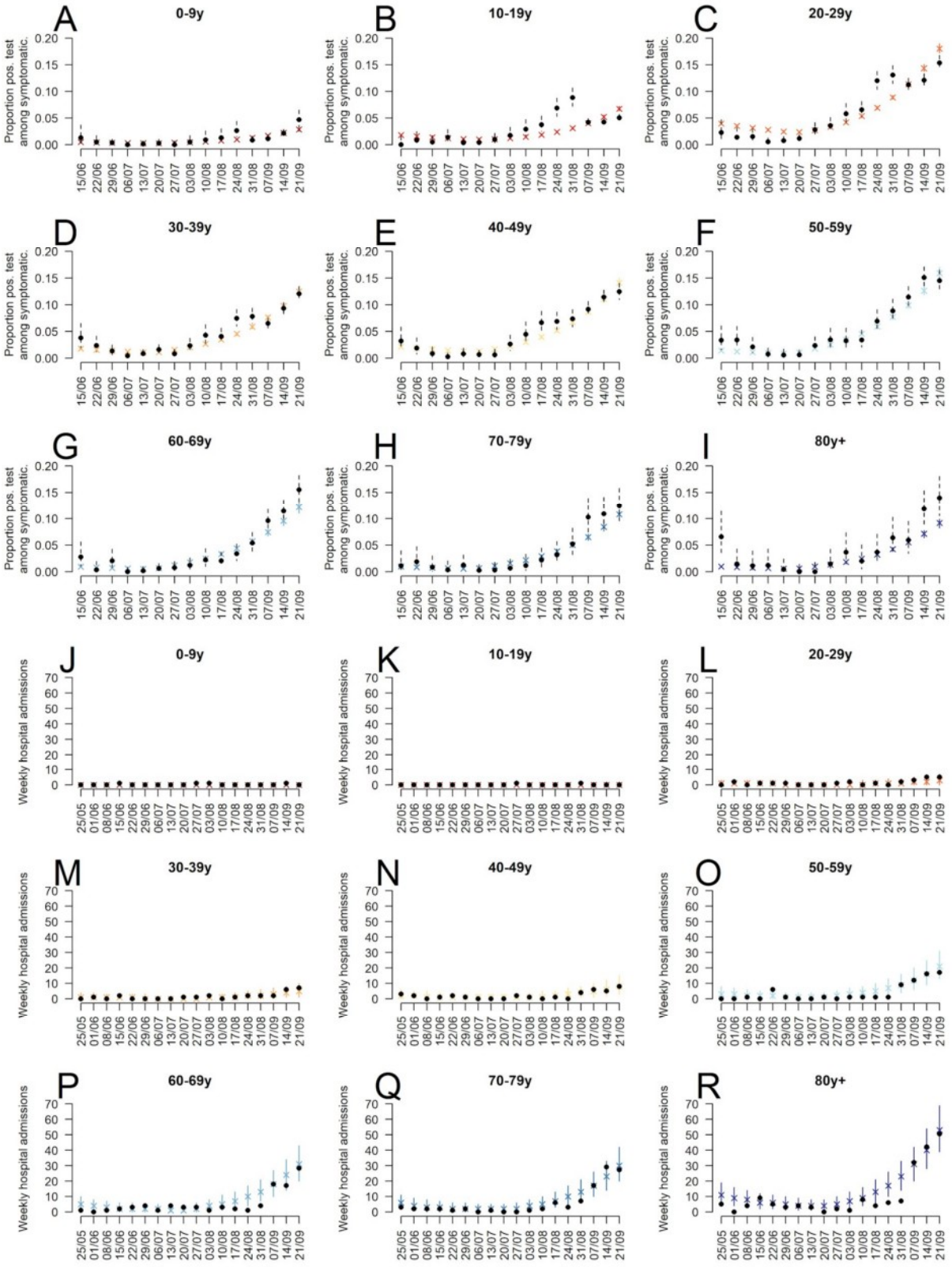

Figure S19: Model predictions and observations in the Occitanie region

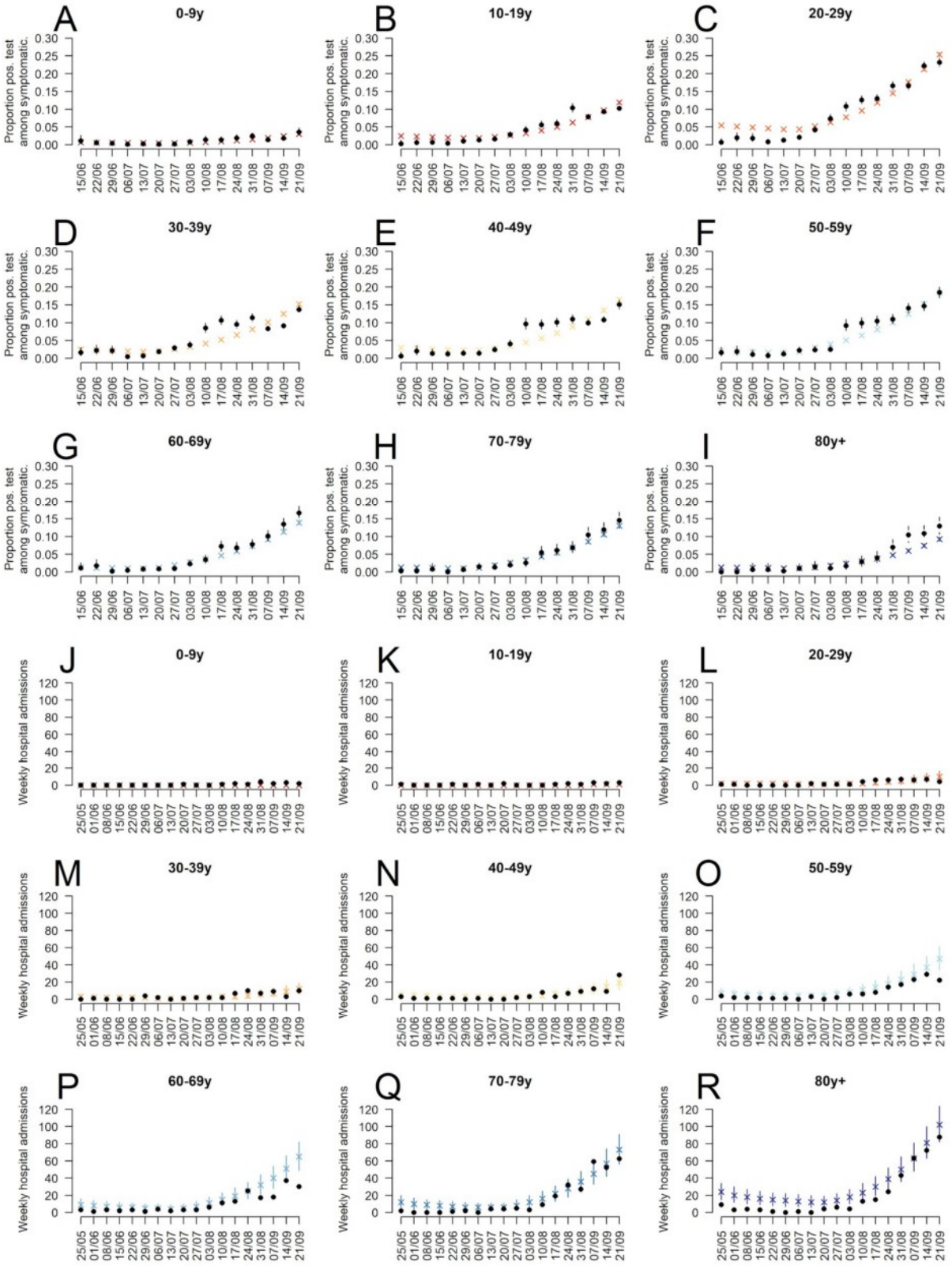

Figure S20: Model predictions and observations in Provence-Alpes Côte d'Azur

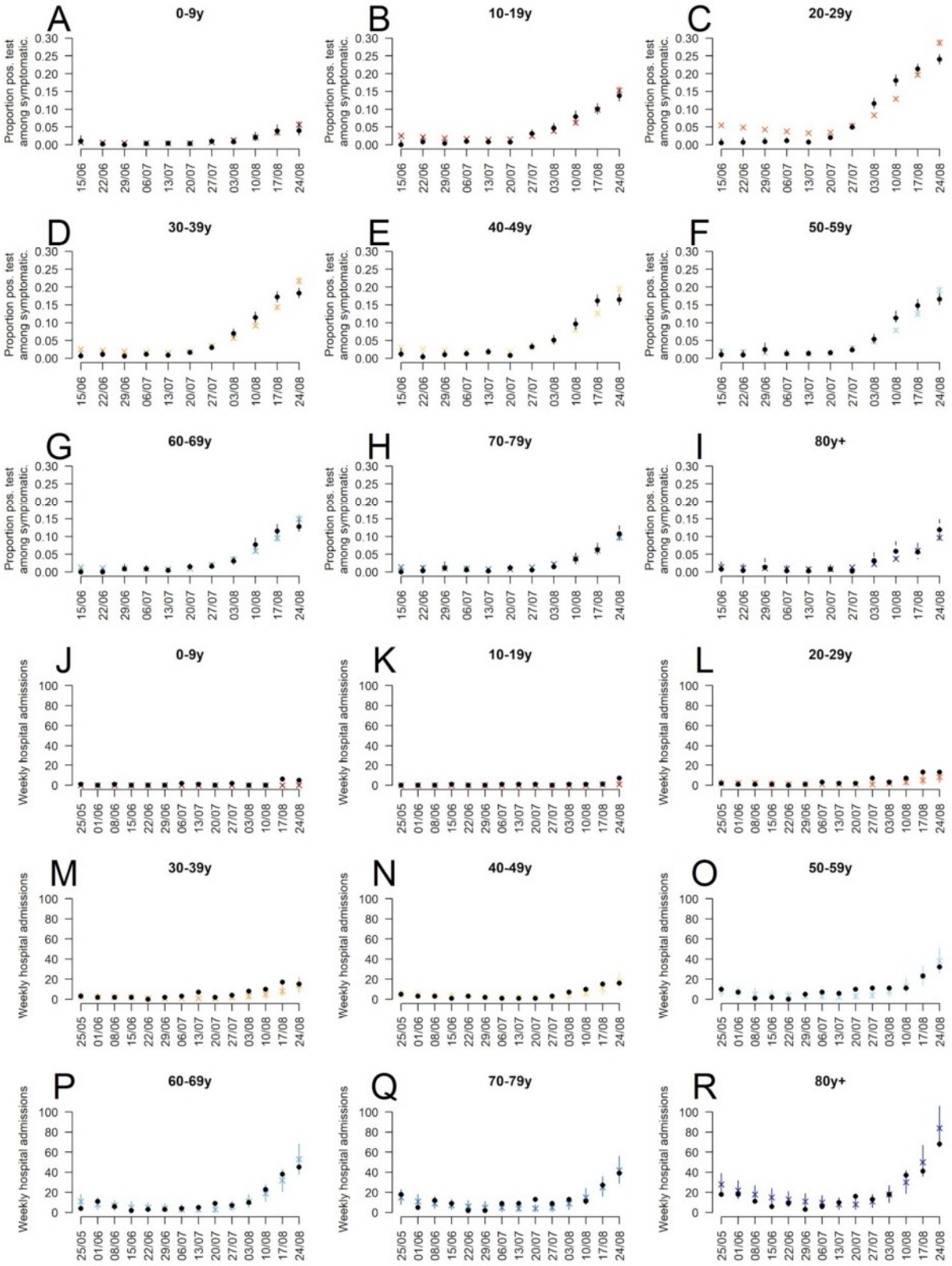

Figure S21: Model predictions and observations in the Pays de la Loire region

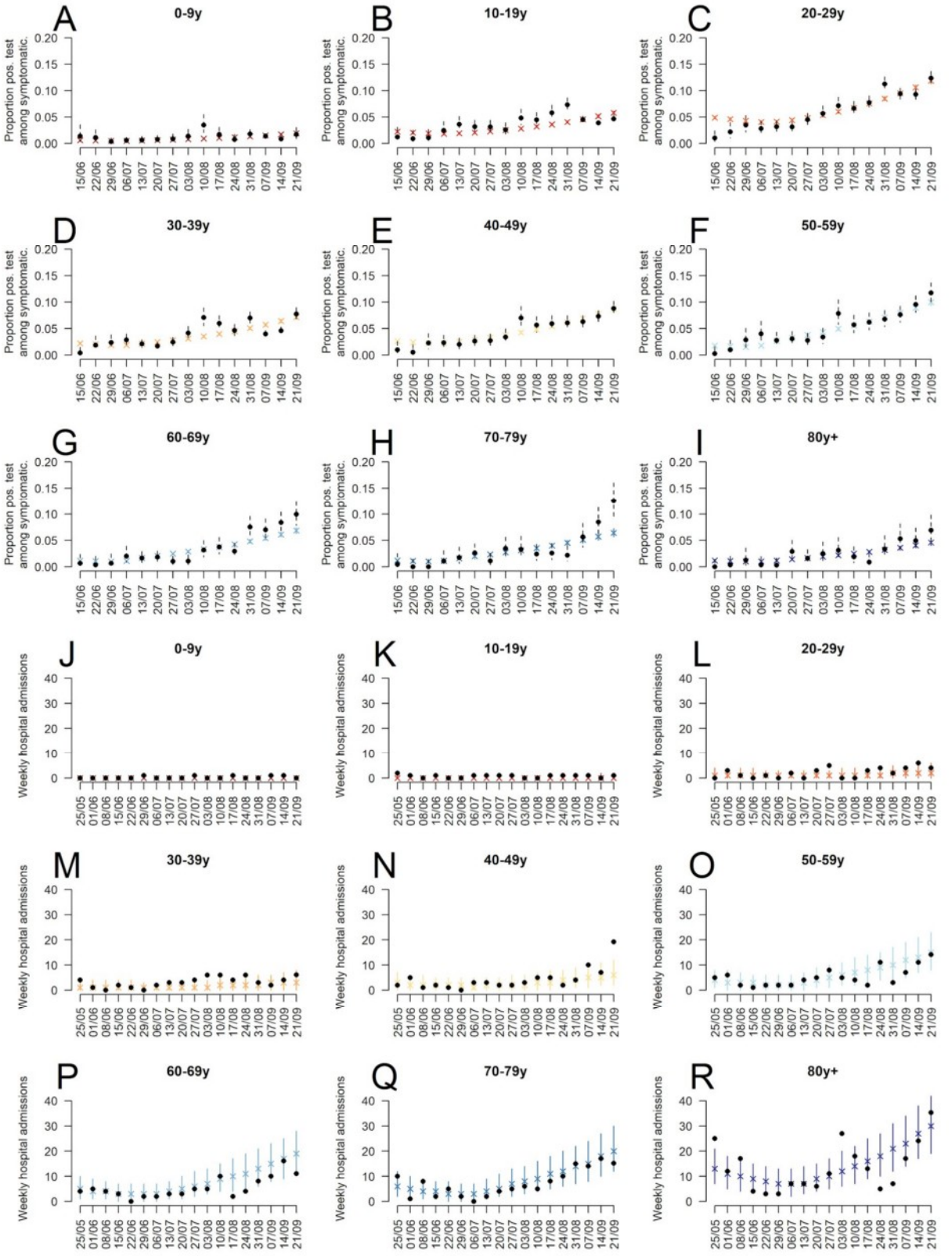

Figure S22

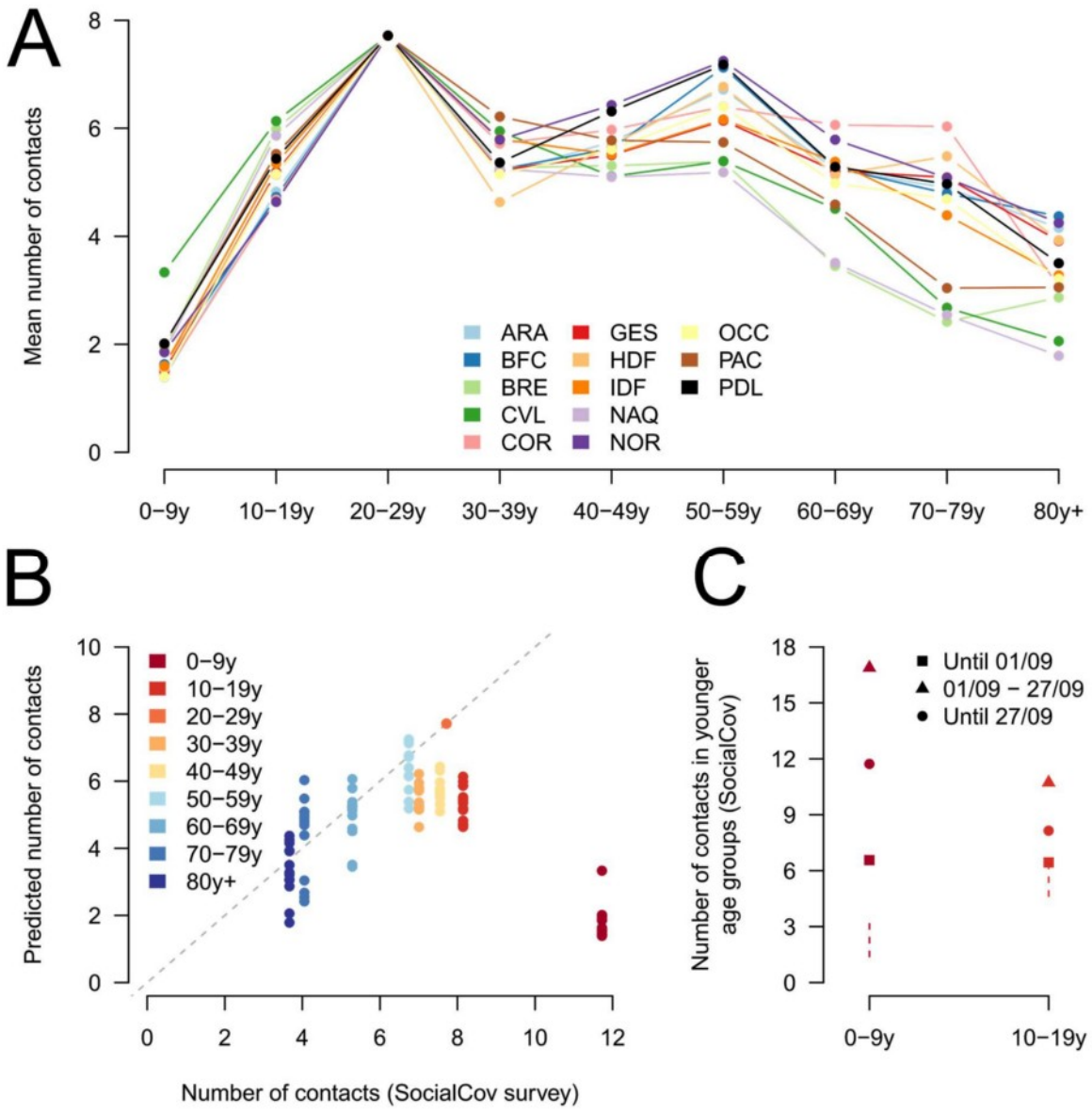

Figure S22: Estimates of the number of contacts during the rebound period in the 13 regions of Metropolitan France (A) Predicted number of contacts in the different age groups during the rebound period. **(B)** Predicted number of contacts in the different age groups during the rebound period and number of contacts extracted from the SocialCov questionnaire between 30 July and 27 September 2020. Each point corresponds to the predictions for one of the 13 metropolitan French regions. **(C)** Number of contacts in the age groups 0-9 y.o. and 10-19 y.o. extracted from the SocialCov survey before the start before 1 September 2020, between 1 September and 27 September 2020 and before 27

September 2020. The dotted segments indicate the ranges of contacts predicted by our model for those two age groups. ARA: Auvergne-Rhônes-Alpes ; BFC: Bourgogne-Franche-Comté ; BRE: Bretagne ; CVL: Centre Val de Loire ; COR: Corse ; GES: Grand Est ; HDF: Hauts-de-France; IDF: Île-de-France; NAQ: Nouvelle-Aquitaine; NOR: Normandie; OCC: Occitanie; PAC: Provence Alpes Côte d'Azur; PDL: Pays de la Loire.

Figure S23

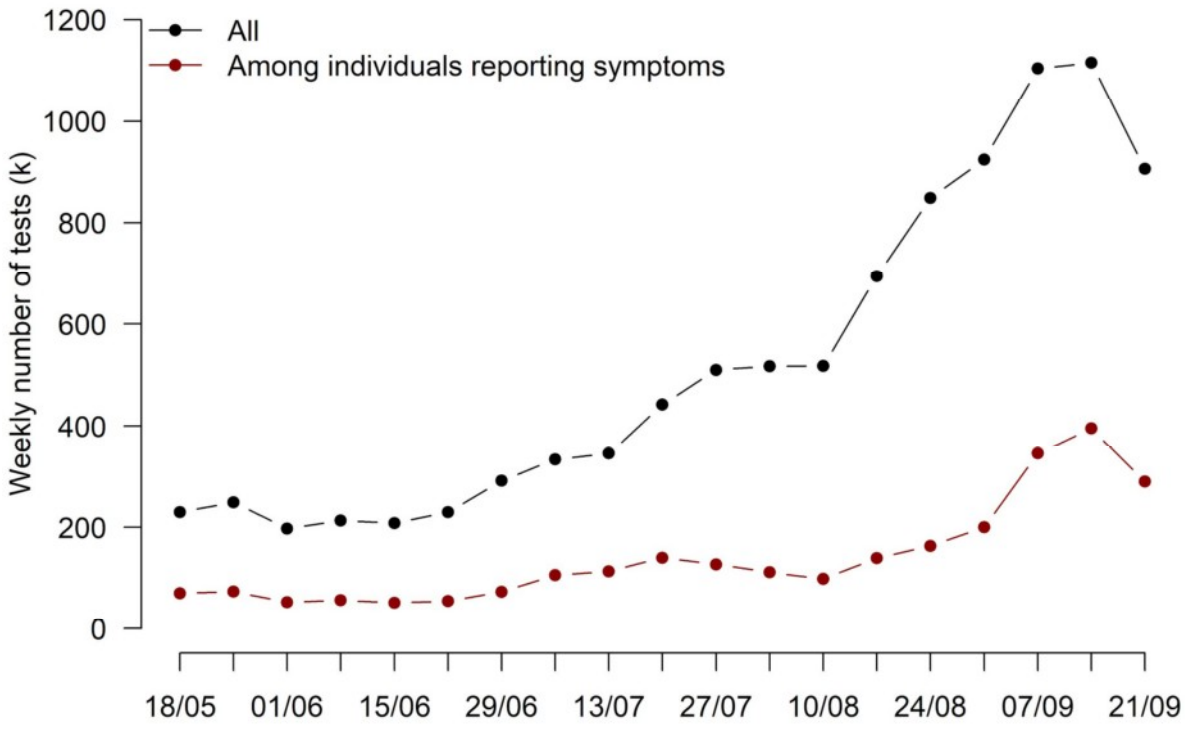

Figure S23: Number of tests performed per week reported in the SIDEP surveillance system in metropolitan France.

Figure S24

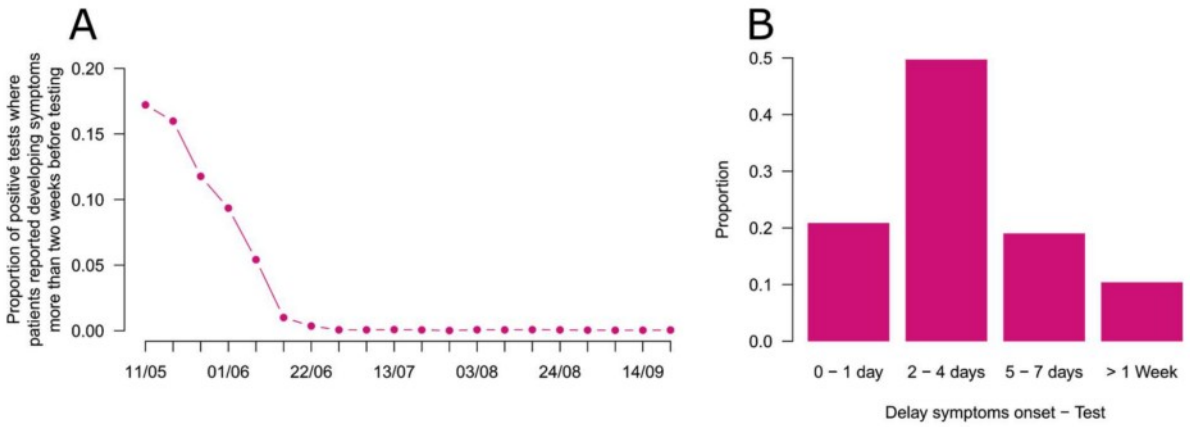

Figure S24: Characteristics of the delay between onset of symptoms and test. (A) Proportion of positive tests in patients reporting a delay greater than two weeks between symptoms onset more and testing by week of nasopharyngeal swab. **(B)** Distribution of the delay between symptoms onset and test for the time period 15 June 2020 - 27 September 2020.

Figure S25

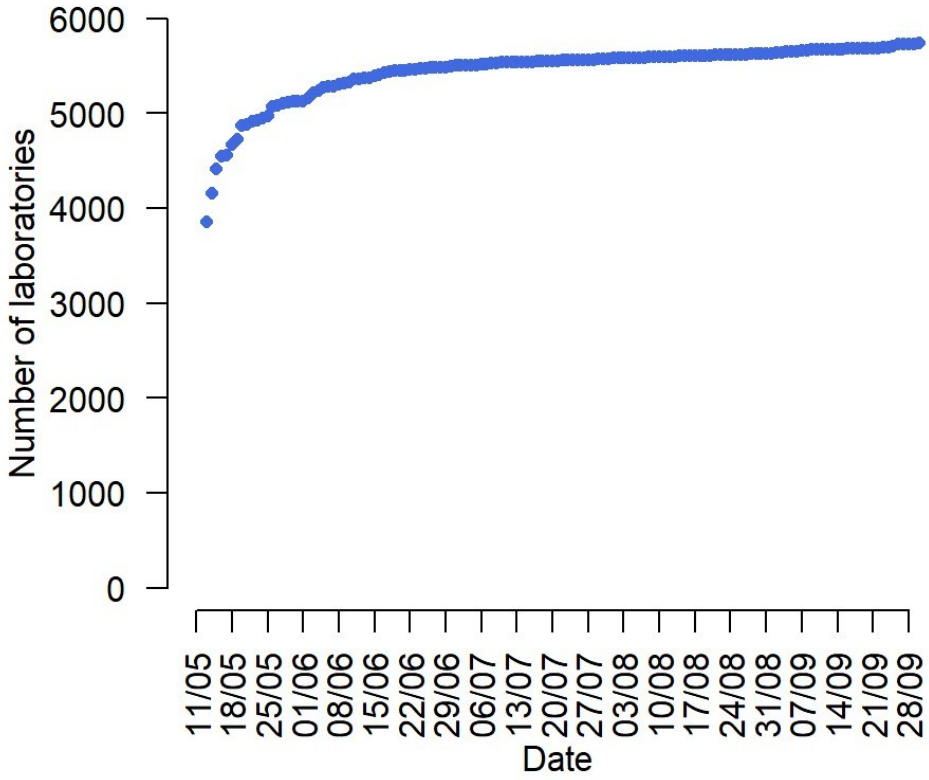

Figure S25: Number of laboratories reporting in the SIDEP database through time.

Table S1: Parameter 95% credible intervals

Parameters common to all the regions

Change in contact patterns during the post-lockdown period for individuals aged 0-9 y.o. $\alpha_{0-9y}{}^{postLock}$	0.18 [0.16 - 0.20]
Change in contact patterns during the post-lockdown period for individuals aged 10-19 y.o.$\alpha_{10-19y}{}^{postLock}$	0.32 [0.30 - 0.34]
Change in contact patterns during the post-lockdown period for individuals aged 30-39 y.o.$\alpha_{30-39y}{}^{postLock}$	0.51 [0.46 - 0.56]
Change in contact patterns during the post-lockdown period for individuals aged 40-49 y.o.$\alpha_{40-49y}{}^{postLock}$	0.55 [0.47 - 0.63]
Change in contact patterns during the post-lockdown period for individuals aged 50-59 y.o.$\alpha_{50-59y}{}^{postLock}$	0.39 [0.36 - 0.43]
Change in contact patterns during the post-lockdown period for individuals aged 60-69 y.o.$\alpha_{60-69y}{}^{postLock}$	0.45 [0.41 - 0.49]
Change in contact patterns during the post-lockdown period for individuals aged 70-79 y.o.$\alpha_{70-79y}{}^{postLock}$	0.45 [0.401 - 0.49]
Change in contact patterns during the post-lockdown period for individuals aged > 80 y.o.$\alpha_{80y+}{}^{postLock}$	0.48 [0.44 - 0.53]
Ratio between the probability of developing symptoms given SARS-CoV-2 infection and the prevalence of non-COVID infections with COVID suggestive symptoms in the population $\gamma/1000$	0.0973 [0.0957 - 0.0996]

Region-specific transmission parameters

Region	Post-lockdown reproduction number $R_{postLock}$	Epidemic rebound reproduction number $R_{rebound}$
ARA	0.87 [0.86 - 0.88]	1.37 [1.36 - 1.37]
BFC	0.88 [0.87 - 0.89]	1.4 [1.38 - 1.41]
BRE	0.85 [0.84 - 0.86]	1.34 [1.32 - 1.36]

CVL	0.84 [0.82 - 0.86]	1.46 [1.43 - 1.5]
COR	1.01 [0.99 - 1.02]	1.28 [1.24 - 1.33]
GES	0.87 [0.86 - 0.88]	1.33 [1.32 - 1.34]
HDF	0.89 [0.89 - 0.9]	1.33 [1.32 - 1.33]
IDF	0.92 [0.91 - 0.93]	1.39 [1.39 - 1.4]
NAQ	0.9 [0.89 - 0.91]	1.7 [1.67 - 1.72]
NOR	0.9 [0.89 - 0.91]	1.35 [1.33 - 1.36]
OCC	0.97 [0.96 - 0.97]	1.31 [1.3 - 1.31]
PAC	0.91 [0.9 - 0.92]	1.68 [1.66 - 1.7]
PDL	0.95 [0.94 - 0.96]	1.17 [1.16 - 1.18]

Region-specific contact parameters $\alpha_{Age}{}^{rebound}$

	Age-group								
Region	0-9y	10-19y	20-29y	30-39y	40-49y	50-59y	60-69y	70-79y	80y+
ARA	0.15 [0.14 - 0.16]	0.31 [0.3 - 0.32]	1 (ref)	0.6 [0.58 - 0.63]	0.55 [0.53 - 0.57]	0.8 [0.76 - 0.86]	1.1 [0.99 - 1.21]	0.86 [0.78 - 0.94]	0.69 [0.64 - 0.74]
BFC	0.18 [0.15 - 0.21]	0.31 [0.29 - 0.33]	1 (ref)	0.63 [0.57 - 0.7]	0.55 [0.5 - 0.6]	0.91 [0.79 - 1.07]	1.11 [0.91 - 1.37]	0.83 [0.68 - 1.08]	0.75 [0.64 - 0.9]
BRE	0.19 [0.15 - 0.24]	0.36 [0.33 - 0.39]	1 (ref)	0.6 [0.51 - 0.71]	0.47 [0.41 - 0.54]	0.55 [0.45 - 0.71]	0.52 [0.42 - 0.69]	0.33 [0.25 - 0.42]	0.43 [0.33 - 0.57]
CVL	0.35 [0.25 - 0.47]	0.38 [0.34 - 0.43]	1 (ref)	0.74 [0.61 - 0.91]	0.46 [0.38 - 0.55]	0.59 [0.47 - 0.75]	0.88 [0.65 - 1.22]	0.39 [0.28 - 0.52]	0.3 [0.22 - 0.4]
COR	0.16 [0.09 -	0.31 [0.25 -	1 (ref)	0.71 [0.55 -	0.58 [0.47 -	0.74 [0.54 -	1.44 [0.97 -	1.39 [0.83 -	0.49 [0.3 - 0.81]

	0.25]	0.38]		0.94]	0.75]	1.05]	2.01]	2.46]	
GES	0.16 [0.14 - 0.18]	0.33 [0.31 - 0.34]	1 (ref)	0.6 [0.56 - 0.66]	0.51 [0.48 - 0.54]	0.68 [0.61 - 0.76]	1.08 [0.93 - 1.25]	0.95 [0.79 - 1.2]	0.62 [0.54 - 0.72]
HDF	0.17 [0.15 - 0.18]	0.33 [0.32 - 0.34]	1 (ref)	0.52 [0.5 - 0.55]	0.54 [0.52 - 0.57]	0.85 [0.78 - 0.91]	1.03 [0.94 - 1.14]	1.17 [0.97 - 1.45]	0.65 [0.58 - 0.71]
IDF	0.17 [0.16 - 0.18]	0.35 [0.34 - 0.35]	1 (ref)	0.72 [0.7 - 0.74]	0.52 [0.51 - 0.54]	0.69 [0.66 - 0.72]	1.22 [1.15 - 1.29]	0.71 [0.66 - 0.76]	0.51 [0.49 - 0.54]
NAQ	0.18 [0.15 - 0.22]	0.35 [0.33 - 0.36]	1 (ref)	0.61 [0.55 - 0.67]	0.44 [0.41 - 0.47]	0.54 [0.48 - 0.61]	0.54 [0.47 - 0.65]	0.35 [0.3 - 0.4]	0.25 [0.21 - 0.29]
NOR	0.21 [0.18 - 0.25]	0.32 [0.3 - 0.34]	1 (ref)	0.73 [0.66 - 0.8]	0.66 [0.61 - 0.71]	0.92 [0.8 - 1.07]	1.38 [1.12 - 1.61]	0.91 [0.74 - 1.17]	0.73 [0.64 - 0.85]
OCC	0.15 [0.13 - 0.17]	0.33 [0.32 - 0.34]	1 (ref)	0.6 [0.57 - 0.63]	0.53 [0.5 - 0.55]	0.75 [0.7 - 0.81]	0.99 [0.89 - 1.12]	0.82 [0.73 - 0.92]	0.5 [0.46 - 0.54]
PAC	0.22 [0.18 - 0.26]	0.36 [0.34 - 0.38]	1 (ref)	0.81 [0.75 - 0.88]	0.55 [0.52 - 0.6]	0.63 [0.57 - 0.7]	0.87 [0.76 - 1.03]	0.45 [0.4 - 0.51]	0.48 [0.43 - 0.55]
PDL	0.23 [0.2 - 0.27]	0.37 [0.35 - 0.39]	1 (ref)	0.65 [0.6 - 0.72]	0.64 [0.59 - 0.7]	0.95 [0.83 - 1.09]	1.13 [0.94 - 1.38]	0.91 [0.76 - 1.21]	0.58 [0.52 - 0.66]

Table S2: Mean daily number of contacts reported by participants of the SocialCov survey between 30 July 2020 and 27 September 2020.

Age group	Mean daily number of contacts (standard error)	Number of answers used to compute the rates
0-9 y.o.	11.7 (0.9)	138
10-19 y.o.	8.1 (0.7)	146
20-29 y.o.	7.7 (0.4)	278
30-39 y.o.	7.0 (0.4)	269
40-49 y.o.	7.5 (0.4)	267
50-59 y.o.	6.7 (0.5)	222
60-69 y.o.	5.3 (0.5)	147
70-79 y.o.	4.1 (0.6)	74
>80 y.o.	3.7 (1.4)	9

Table S3: Change in the probability of ICU admission given hospitalization

Age-group	Time window		
	T1: 13 March – 10 May	T2: 11 May – 12 July	T3: 13 July – 30 September
0-39 y.o.	Ref	1.01 [0.83,1.2]	0.9 [0.79,1.01]
40-49 y.o.	Ref	0.76 [0.6,0.93]	0.89 [0.79,1]
50-59 y.o.	Ref	0.75 [0.63,0.87]	0.97 [0.89,1.04]
60-69 y.o.	Ref	0.67 [0.58,0.76]	0.98 [0.92,1.04]
70-79 y.o.	Ref	0.66 [0.58,0.75]	1.16 [1.09,1.23]
> 80 y.o.	Ref	1.21 [1.04,1.4]	2.18 [1.98,2.39]

Table S4: Change in the probability of death given hospitalization through time.

Age-group	Time window		
	T1: 13 March – 10 May	T2: 11 May – 12 July	T3: 13 July – 30 September
0-39 y.o.	Ref	0.8 [0.37,1.41]	0.43 [0.22,0.73]
40-49 y.o.	Ref	1.17 [0.68,1.8]	0.48 [0.27,0.74]
50-59 y.o.	Ref	0.78 [0.54,1.04]	0.4 [0.28,0.53]
60-69 y.o.	Ref	0.66 [0.53,0.8]	0.33 [0.27,0.41]
70-79 y.o.	Ref	0.48 [0.41,0.56]	0.5 [0.44,0.57]
> 80 y.o.	Ref	0.55 [0.5,0.59]	0.66 [0.62,0.7]

Table S5: Adjusted probabilities of ICU admission and death given hospitalization used in forward simulations.

Age-group	Probability of ICU admission given hospitalization	Probability of death given hospitalization
0-19 y.o.	20.0%	0.3%
20-29 y.o.	10.4%	0.5%
30-39 y.o.	14.3%	0.8%
40-49 y.o.	19.8%	1.6%
50-59 y.o.	26.7%	2.6%
60-69 y.o.	30.2%	4.2%
70-79 y.o.	28.9%	10.5%
> 80 y.o.	12.2%	20.9%

Table S6: Percentage of hospital deaths arising among patients hospitalized in ICUs.

Age-group	Time window		
	T1: 13 March – 10 May	T2: 11 May – 12 July	T3: 13 July – 30 September
0-39 y.o.	72.1 [63.6,79.6]	53.6 [25.9,81.8]	66.1 [40,86.4]
40-49 y.o.	62.9 [56.5,69]	55.7 [32.7,77.7]	60.5 [37.3,81.5]
50-59 y.o.	62.4 [59,65.7]	34.8 [20.3,50.6]	72.9 [59.3,84.7]
60-69 y.o.	57.4 [55.4,59.5]	54.1 [43.5,64.4]	63.3 [53.5,72.3]
70-79 y.o.	39.4 [37.9,40.8]	39.6 [31.6,47.8]	60.8 [55.1,66.4]
> 80 y.o.	7.6 [7.1,8.2]	11.4 [8.9,14.2]	19.5 [16.7,22.4]

Table S7: Dates used for a change in transmission levels in regions in Metropolitan France.

Region	Date
Auvergne-Rhône-Alpes	09/07/2020
Bourgogne-Franche-Comté	23/07/2020
Bretagne	06/07/2020
Centre-Val de Loire	09/07/2020
Corse	06/08/2020
Grand Est	09/07/2020
Hauts-de-France	09/07/2020
Île-de-France	25/06/2020
Nouvelle-Aquitaine	23/07/2020
Normandie	17/07/2020
Occitanie	17/07/2020
Provence Alpes Côte d'Azur	17/07/2020
Pays de la Loire	03/07/2020

Table S8: Time windows used to calibrate the model in the different regions

Region	Time window
Auvergne-Rhône-Alpes	11/05/2020 - 27/09/2020
Bourgogne-Franche-Comté	11/05/2020 - 27/09/2020
Bretagne	11/05/2020 - 06/09/2020
Centre-Val de Loire	11/05/2020 - 31/08/2020
Corse	11/05/2020 - 27/09/2020
Grand Est	11/05/2020 - 27/09/2020
Hauts-de-France	11/05/2020 - 27/09/2020
Île-de-France	11/05/2020 - 27/09/2020
Nouvelle-Aquitaine	11/05/2020 - 06/09/2020
Normandie	11/05/2020 - 27/09/2020
Occitanie	11/05/2020 - 27/09/2020
Provence Alpes Côte d'Azur	11/05/2020 - 31/08/2020
Pays de la Loire	11/05/2020 - 27/09/2020

Table S9: Weights used to compute the number of life years lost and the number of quality adjusted life years lost.

Age group	Weights for the computation of the number of life years lost	Weights for the computation of the number of quality adjusted life years lost
0-9 y.o.	78.4 years	66.6 years
10-19 y.o.	65.5 years	56.7 years
20-29 y.o.	58.7 years	47.2 years
30-39 y.o.	49.0 years	38.5 years
40-49 y.o.	39.4 years	30.3 years
50-59 y.o.	30.4 years	22.9 years
60-69 y.o.	22.1 years	16.2 years
70-79 y.o.	14.4 years	10.3 years
> 80 y.o.	6.9 years	4.9 years